

**Special Section:**

Atlantic Meridional  
Overturning Circulation:  
Reviews of Observational and  
Modeling Advances

**Key Points:**

- Lagrangian methods are critical to describing the three-dimensional structure of the Atlantic Meridional Overturning Circulation
- Fluid parcel trajectories reveal the lack of meridional connectivity in both the shallow and deep limbs of the overturning circulation
- High spatial-temporal resolution trajectories identify regions where coherent eddies contribute to the overturning circulation

**Correspondence to:**

A. Bower,  
abower@whoi.edu

**Citation:**

Bower, A., Lozier, S., Biastoch, A., Drouin, K., Foukal, N., Furey, H., et al. (2019). Lagrangian views of the pathways of the Atlantic Meridional Overturning Circulation. *Journal of Geophysical Research: Oceans*, 124, 5313–5335. <https://doi.org/10.1029/2019JC015014>

Received 30 JAN 2019

Accepted 8 JUL 2019

Accepted article online 19 JUL 2019

Published online 15 AUG 2019

©2019. The Authors.

This is an open access article under the terms of the Creative Commons Attribution-NonCommercial-NoDerivs License, which permits use and distribution in any medium, provided the original work is properly cited, the use is non-commercial and no modifications or adaptations are made.

## Lagrangian Views of the Pathways of the Atlantic Meridional Overturning Circulation

A. Bower<sup>1</sup> , S. Lozier<sup>2,3</sup> , A. Biastoch<sup>4</sup> , K. Drouin<sup>2</sup> , N. Foukal<sup>1</sup> , H. Furey<sup>1</sup> , M. Lankhorst<sup>5</sup> , S. Rühs<sup>6</sup> , and S. Zou<sup>2,7</sup> 

<sup>1</sup>Woods Hole, Oceanographic Institution, Woods Hole, MA, USA, <sup>2</sup>Department of Earth and Ocean Sciences, Duke University, Durham, NC, USA, <sup>3</sup>Now at Department of Earth and Atmospheric Sciences, Georgia Institute of Technology, Atlanta, GA, USA, <sup>4</sup>GEOMAR Helmholtz Centre for Ocean Research Kiel, Kiel, Germany, <sup>5</sup>Scripps Institution of Oceanography, University of California San Diego, La Jolla, CA, USA, <sup>6</sup>Ocean Frontier Institute Dalhousie University, Halifax, Nova Scotia, Canada, <sup>7</sup>Now at Department of Physical Oceanography, Woods Hole Oceanographic Institution, Woods Hole, MA, USA

**Abstract** The Lagrangian method—where current location and intensity are determined by tracking the movement of flow along its path—is the oldest technique for measuring the ocean circulation. For centuries, mariners used compilations of ship drift data to map out the location and intensity of surface currents along major shipping routes of the global ocean. In the mid-20th century, technological advances in electronic navigation allowed oceanographers to continuously track freely drifting surface buoys throughout the ice-free oceans and begin to construct basin-scale, and eventually global-scale, maps of the surface circulation. At about the same time, development of acoustic methods to track neutrally buoyant floats below the surface led to important new discoveries regarding the deep circulation. Since then, Lagrangian observing and modeling techniques have been used to explore the structure of the general circulation and its variability throughout the global ocean, but especially in the Atlantic Ocean. In this review, Lagrangian studies that focus on pathways of the upper and lower limbs of the Atlantic Meridional Overturning Circulation (AMOC), both observational and numerical, have been gathered together to illustrate aspects of the AMOC that are uniquely captured by this technique. These include the importance of horizontal recirculation gyres and interior (as opposed to boundary) pathways, the connectivity (or lack thereof) of the AMOC across latitudes, and the role of mesoscale eddies in some regions as the primary AMOC transport mechanism. There remain vast areas of the deep ocean where there are no direct observations of the pathways of the AMOC.

**Plain Language Summary** Measuring ocean currents by following their paths—rather than by observing them at a fixed location—is the oldest method for exploring ocean currents. For centuries, mariners used compilations of ship drift data to map out the location and intensity of surface currents along major shipping routes of the global ocean. In the mid-20th century, technological advances in electronic navigation allowed oceanographers to track freely drifting surface buoys continuously throughout the ice-free oceans and begin to construct global maps of the surface currents. At about the same time, the development of methods using sound to track floats below the surface led to important new discoveries regarding the currents bar below the surface. Since then, these techniques have been used to explore the location and strength of currents, and how they change in time, throughout the world's oceans, but especially in the Atlantic Ocean. Computer simulations of the oceans are also used to calculate the pathways of virtual surface drifters and subsurface floats. In this review, studies that use these flow-following methods to measure the pathways of the north-south shallow and deep currents that make up the Atlantic Meridional Overturning Circulation (also sometimes referred to as the Great Ocean Conveyor) have been gathered together to illustrate aspects of the conveyor system that are uniquely captured by this technique. These include the importance of large recirculations, or “waiting areas,” where water circulates around and around before moving onto the next segment of the conveyor. Also, these techniques for observing ocean currents illustrate how disconnected some parts of the conveyor are, and how swirling, translating pools of water ~100 km in diameter, and not continuous currents, help to move water along the conveyor's path. Vast areas of the deep ocean remain where there are no direct observations of the pathways of the conveyor.

### 1. Introduction

The Atlantic Meridional Overturning Circulation (AMOC) refers to the net northward transport of relatively warm, low-density upper-ocean waters from the South Atlantic (SA) to the high latitudes of the North

Atlantic and Nordic Seas (Norwegian, Greenland, and Iceland Seas), where they lose heat to the atmosphere and become colder and denser. The transformed water masses, historically referred to collectively as North Atlantic Deep Water (NADW) are transported back southward in (approximately) equal measure to the net northward transport. The AMOC is a key component of the Earth's climate system (Intergovernmental Panel on Climate Change Fifth Assessment Report, 2014). For example, at subtropical latitudes in the North Atlantic, the AMOC is responsible for about a quarter of the total northward heat flux transported by the ocean and atmosphere combined (Trenberth & Caron, 2001). Interannual and longer time scale AMOC variability has been linked to North Atlantic sea surface temperature and hence to climate variability in Europe and North America, African rainfall, Atlantic hurricane activity, Arctic sea ice coverage, and atmospheric carbon sequestration (Lozier et al., 2017 and references therein).

Given its importance to climate variability and related societal concerns, determining the mean state of the AMOC and its past and present changes are high priorities in the oceanographic community (Cunningham et al., 2010) but a daunting observational challenge. Measuring the mass, heat, and fresh water fluxes associated with the AMOC requires transbasin observations of the currents, temperature, and salinity from sea surface to sea floor. Synoptic AMOC estimates can be derived from single transbasin hydrographic sections, although necessary assumptions about reference levels add uncertainty to these estimates, and they may not resolve the most important time scales of variability (Bryden et al., 2005; Srokosz & Bryden, 2015). Continuous monitoring of the AMOC has been achieved at several latitudes in the 21st century, with moored trans-basin observing systems that include a combination of direct and indirect measures of top-to-bottom currents, along with temperature and salinity (Cunningham et al., 2007; Lozier et al., 2019; Meinen et al., 2018; Send et al., 2011; Willis, 2010). These pioneering efforts have already revealed surprising results, including the significant impact of wind-forcing on seasonal-to-interannual time scales (e.g., Zhao & Johns, 2014), and the disassociation between AMOC variability and dense water formation in the Labrador Sea on interannual time scales (Lozier et al., 2019).

While such observing systems are critical for developing a solid understanding of the linkages between dense water formation, wind forcing, and AMOC variability, they typically do not inform us on the three-dimensional structure of the AMOC. The iconic depiction of the global (and Atlantic) MOC as a single conveyor belt (Broecker, 1991) has been valuable for bringing attention to scientists and the public alike regarding the connectivity of the global ocean circulation, but if taken too literally, it perpetuates a vast oversimplification of the complex system of currents that together make up the AMOC. It can also unintentionally give the impression that the AMOC is a tightly connected system where changes in one part are more or less instantly communicated to the rest of the system. The Lagrangian approach to observing ocean circulation is helping to overcome both of these potential misperceptions—by tracing the pathways of fluid parcels over long distances, new pathways of the AMOC have been discovered, and the connectivity of the AMOC pathways within and between hemispheres and gyres has been assessed.

The very first quantitative measurements of ocean currents were Lagrangian, based on the deviation of ships off their intended course, and short-term visual tracking of drifting objects released either on purpose or accidentally (Richardson, 2019). With the development of satellite-based positioning systems in the 1970s, surface drifters could be tracked continuously and autonomously for thousands of kilometers over many months. Tens of thousands of surface drifters have since been deployed.

Some of the first direct *subsurface* current observations were also Lagrangian, made by tracking sealed and carefully ballasted scaffolding pipes equipped with an acoustic pinger from a research vessel, to confirm a theoretical conjecture that there was a deep (~3,000 m) equatorward flowing current along the western boundary of the North Atlantic, the Deep Western Boundary Current (DWBC; Stommel, 1957, 1958; Swallow & Worthington, 1957, 1961; Gould, 2005). The 1960 release of a number of similar floats west of Bermuda from the sailing vessel *Aries* revealed for the first time the existence of energetic mesoscale eddies in the deep ocean. The surprising dispersion of the floats in all directions by the eddy field made it immediately apparent that ship-based float tracking was impractical and insufficient to map out the subsurface ocean circulation over larger spatial and temporal scales. A long-range acoustic float tracking method was developed by Rossby and Webb (1970), based on an early conceptual idea proposed by Stommel (1955), capitalizing on the ducting effect of the middepth “sound channel”.

They demonstrated that larger metal tubes could be forced to resonate like organ pipes and tracked continuously (with position fixes every day or so) for several years over thousands of kilometers, using fixed listening

stations (hydrophones). Later the direction of the acoustic path was reversed such that now signals from an array of moored sound sources are detected by floats equipped with hydrophones (Rossby, 2016; Rossby et al., 1986). With the high rate of positioning enabled by the acoustic tracking network, the structure and intensity of mesoscale motions and narrow fronts and boundary currents could be resolved.

In the 1980s, profiling floats were developed and added to the Lagrangian toolkit for observing ocean currents (Davis et al., 1992). These floats drift at depths typically between 1,000 and 2,000 m, and periodically (every ~10 days) come to the surface to fix their position with the Global Positioning System and transmit that position as well as vertical profiles of water properties. The average current at depth is determined from the float's displacement vector over the 10 days between surfacings. Without the need for the network of moored sound sources, profiling floats have now been deployed throughout the global oceans as part of the International Argo Program. At the time of writing, more than 3,900 floats are continuously providing their positions and profiles.

All of these long-lived, autonomous Lagrangian platforms are especially useful for mapping the spatial structure of the ocean circulation since the mesoscale eddy field causes them to spread out naturally, providing velocity observations over much larger areas than can be surveyed by ships or instrumented with traditional (Eulerian) moorings fixed to the sea floor. For example, Fratantoni (2001) provided the first basin-wide quantitative analysis of the near-surface circulation of the entire North Atlantic from in situ observations based on the trajectories of 1,500 surface drifters deployed in the 1990s. In large numbers such as these, floats and drifters can be used to map out mean currents over large areas. But even single trajectories are valuable as they may reveal a previously unknown flow pathway or transport mechanism (Ramsey et al., 2018).

Calculating fluid particle trajectories in numerical models provides an important extension to the analysis of necessarily limited numbers of surface drifter and float trajectories. The study of Lagrangian output from eddy-resolving ocean general circulation models got its start in the 1980s (van Sebille et al., 2017). Orders of magnitude more and longer-duration simulated particle trajectories can be calculated from a model's Eulerian velocity fields at relatively low computational cost, verifying inferences drawn from observed trajectories and often adding confidence limits to those inferences. An added benefit of simulated trajectories is the ability to calculate "back trajectories," by integrating the model velocity along a particle trajectory backward in time. This allows us to determine (to the extent that the numerical model represents reasonably well the mean and eddy velocity fields) where fluid particles passing some point came from. This is particularly useful for examining the degree of connectivity and transit times between far-separated branches of the AMOC.

In this review, we highlight what has been learned from Lagrangian studies, both observational and numerical, along the large-scale pathways of the AMOC through the Atlantic Ocean, focusing on meridional connectivity. We begin in section 2 with the entry of upper-limb waters into the SA from the Indian and Pacific Oceans. We follow the upper-limb pathways northward through the SA, across the equator, through the subtropical and subpolar North Atlantic and into the Nordic Seas. Transport estimates—a few derived from Lagrangian analysis, most by other methods—are provided where available to give some context, but the focus is on the pathways and mechanisms by which the waters of the upper limb of the AMOC make their way northward. The review continues in section 3 with a synthesis of Lagrangian studies of the lower-limb AMOC, beginning with the pathways of dense waters in the Nordic Seas as they approach the shallow sills of the Greenland-Scotland Ridge, along their descent into and through the subpolar and subtropical North Atlantic, southward across the equator, and through the SA. In section 4, we provide some conclusions and the future outlook. Figure 1 works both as a reference for the currents referred to in the following sections and as a summary of the various pathways and processes revealed by Lagrangian observations and model-derived simulated particle trajectories.

## 2. AMOC Upper limb

### 2.1. South Atlantic

The upper limb of the SA MOC primarily sources its waters from the Pacific Ocean through Drake Passage and the Indian Ocean via the Agulhas Current System (Figure 2). Traditionally, these pathways have been referred to as the "cold" (Rintoul, 1991) and "warm" water routes (Gordon, 1989), respectively, due to

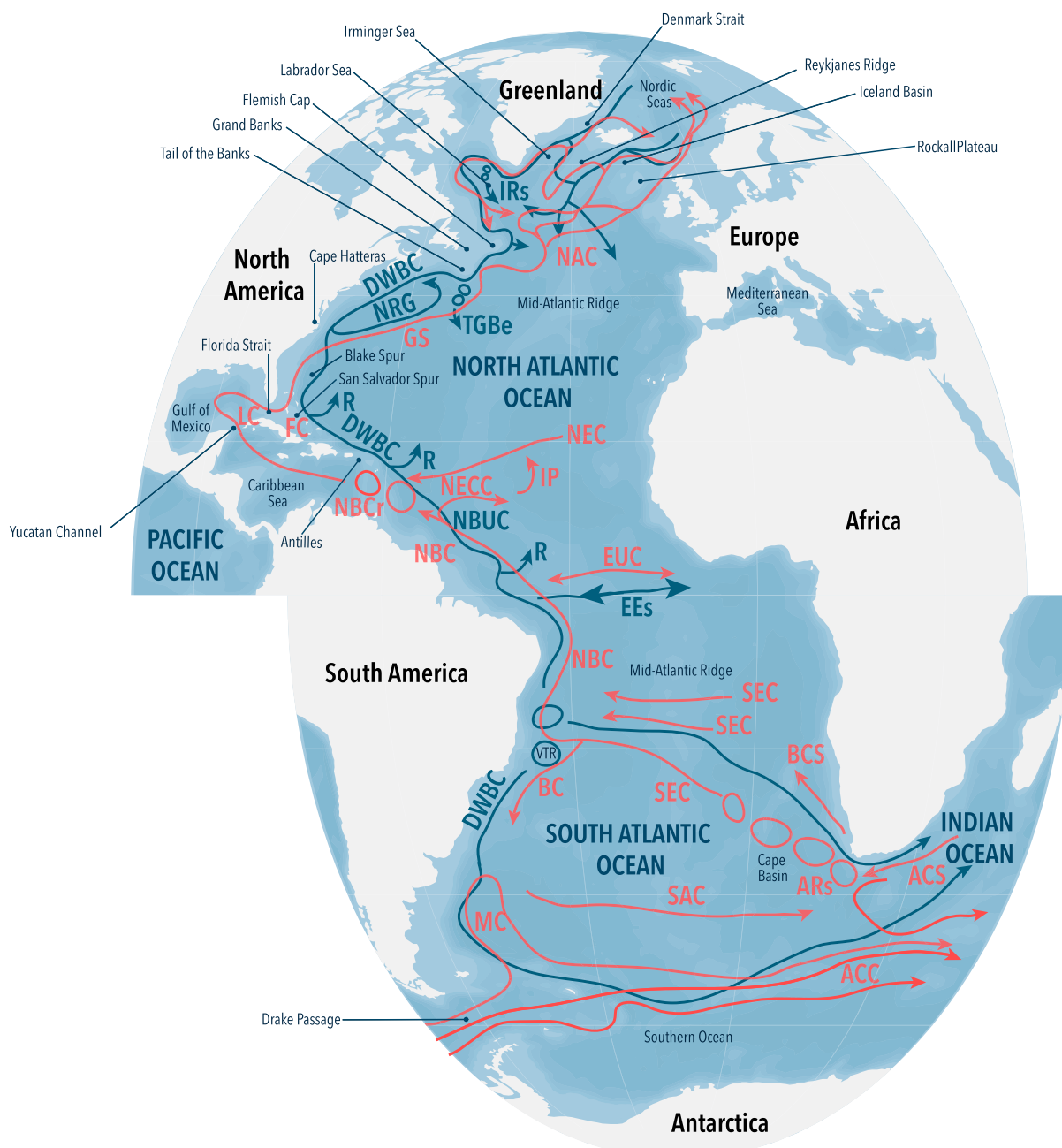


**Figure 1.** Overview of the upper (red) and lower (blue) limbs of the Atlantic Meridional Overturning Circulation as observed by the Lagrangian method. This figure includes most geographic features and currents mentioned in text. Bathymetry is shaded at 1,000-m intervals. In alphabetical order: ACC, Antarctic Circumpolar Current; ACS, Agulhas Current System; ARs, Agulhas Rings; BC, Brazil Current; BCS, Benguela Current System; DWBC, Deep Western Boundary Current; EEs, Equatorial Excursions; EUC, Equatorial Undercurrent; FC, Florida Current; GS, Gulf Stream; IP, interior pathways; IRRs, Irminger Rings; LC, Loop Current; MAR, mid-Atlantic Ridge; MC, Malvinas Current; NAC, North Atlantic Current; NBC, North Brazil Current; NBCr, North Brazil Current Rings; NBUC, North Brazil Undercurrent; NEC, North Equatorial Current; NECC, North Equatorial Counter Current; NRG, Northern Recirculation Gyre; R, recirculation; SAC, South Atlantic Current; SEC, South Equatorial Current; TGBe, Tail of the Grand Bank Eddies.

their inherently different thermohaline properties. However, their relative contributions to the volume transport and properties of the AMOC upper limb remain controversial (Garzoli & Matano, 2011). Over the last two decades research has primarily focused on the contribution of the warm water route, since various studies suggested an increase of Agulhas Leakage since the 1960s (e.g., Biastoch et al., 2009),

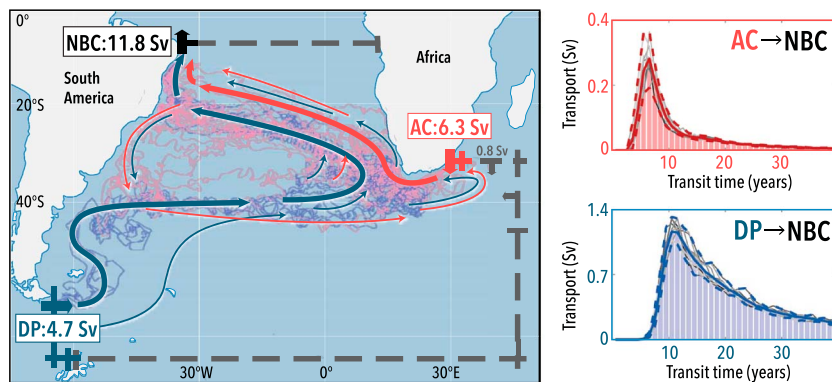


**Figure 2.** SAMOCs upper limb: direct “cold” (blue) and “warm” (red) water routes inferred from  $O(10^6)$  simulated Lagrangian particle trajectories, which were calculated backward from the North Brazil Current (NBC) to the Drake Passage (DP) and Agulhas Current (AC) in an eddy-rich ocean model. (left) Exemplary trajectories (curly thin lines), major/minor (thick/thin arrows) pathways, and time-mean transports. (right) Lagrangian transport-weighted transit-time distributions for the two routes; mean (bars, colored solid lines) distributions of 10 experiments with different particle release years (displayed in thin grey solid lines), as well as their range (dashed). Figure adapted from Rühs et al. (2019).

which could impact the strength of the AMOC through different processes on various timescales (e.g., Beal et al., 2011; Weijer et al., 2002).

The Agulhas Current feeds of relatively warm and salty upper and intermediate waters from the Indian Ocean have recently been discussed in detail by Durgadoo et al. (2017) in a Lagrangian modeling framework. As a strong western boundary current, the Agulhas Current overshoots the African continent before reflecting to the Indian Ocean. Approximately a quarter of its transport “leaks” into the SA in the form of Agulhas rings, filaments, and direct inflow. However, observational estimates of Agulhas leakage remain scarce. Even though Agulhas rings have a diameter of up to 300 km, their deep velocities down to more than 1,000 m prevent the quantification of total leakage from satellite altimetry alone (Casanova-Masjoan et al., 2017; van Aken et al., 2003). Richardson (2007) estimated a 15-Sv leakage in the upper 1,000 m from subsurface floats and surface drifters. More recently, a combination of ARGO float data and satellite altimetry revealed an Agulhas ring transport of  $9 \pm 8$  Sv (Souza et al., 2011). Owing to the intermittent character of ring shedding, Agulhas leakage is subject to strong interannual variability, hence usually studied by means of Lagrangian analysis with ocean models (Biastoch et al., 2009). Hindcast simulations show (multi)decadal variations, with a 30% increase of Agulhas leakage between the 1960s and 2000s associated with changes in the Southern Hemisphere winds (Biastoch et al., 2015; Durgadoo et al., 2013). Lagrangian model analyses further suggest that Agulhas leakage does not exclusively flow directly into the AMOC: about 50% recirculates within the SA’s horizontal gyre circulation (Rühs et al., 2013).

The 134- to 173-Sv inflow from the Drake Passage (Cunningham et al., 2003; Donohue et al., 2016) into the Atlantic sector of the Southern Ocean is composed of relatively cold and fresh intermediate waters, which primarily remain in the Antarctic Circumpolar Current. A small fraction diverts northward into the Malvinas Current and enters the SA subtropical gyre circulation, forming the (direct) cold water route (Friocourt et al., 2005; Speich et al., 2001). Historically, its contribution to the AMOC upper limb was estimated as 1-2 Sv from Lagrangian analyses of relatively coarse, eddy-poor, and eddy-active models (Donners & Drijfhout, 2004; Friocourt et al., 2005; Speich et al., 2001). An additional 4-6 Sv of Drake Passage inflow indirectly contributes to the AMOC upper limb as it exits the SA in the Antarctic Circumpolar Current, recirculates in the Indian Ocean, and eventually forms part of Agulhas leakage (Friocourt et al., 2005; Speich et al., 2001, 2007). Hence, this indirect contribution is counted as part of the warm water route.

Rodrigues et al. (2010) used quasi-isobaric subsurface floats and hydrographic data and estimated a “direct” cold water route contribution of 4.7 Sv (36%) and a warm water route contribution of 8.5 Sv (64%). This finding corresponds well to recent results (cold: 4.7 Sv or 40%; warm: 7.1 Sv or 60%) from Lagrangian analyses in an eddy-rich ocean model by Rühs et al. (2019). The authors also show that water contributing to the upper limb of the AMOC from both routes preferentially follows the South Equatorial Current (SEC) before exiting

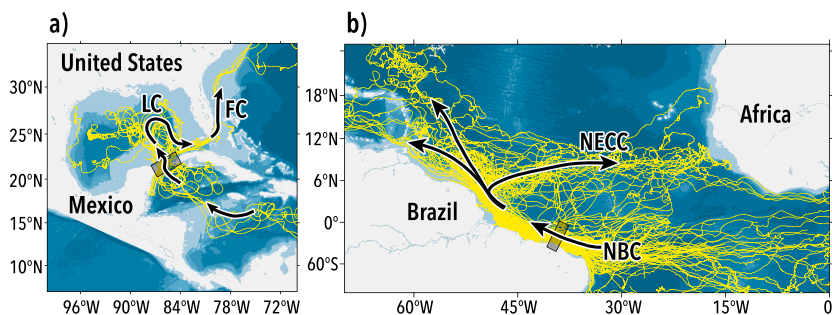


**Figure 3.** Select surface trajectories from the Global Drifter Program (GDP). The selection is for those drifters that pass through a given box (marked on each map), out of a block of 5,000 trajectories (data file for IDs 10001-15000 as distributed by the GDP). (a) Trajectories passing through a box in Yucatan Channel. The inflow from the east through the Caribbean and into the Channel, the Loop Current (LC), and finally the Florida Current (FC) are highlighted by arrows. (b) Trajectories in the North Brazil Current (NBC). The arrows show the inflow from the South Equatorial Current into the NBC, from where successive paths lead directly into the Caribbean, northward but east of the Caribbean, or retroflect into the North Equatorial Countercurrent (NECC). Flow from the North Equatorial Current is not shown. Bottom topography is shaded in 1,000-m intervals.

toward the North Atlantic through the North Brazil Current (NBC). Most prominent timescales to the NBC are on the order of 6–7 years for the warm water route and 12 years for the “direct” cold water route (Rühs et al., 2013; Rühs et al., 2019). Long tails of the age distributions reflect that recirculations, for example, in the subtropical gyre, are also a significant component of AMOC pathways in the SA. Since waters from both sources are subject to interior mixing and strong air-sea fluxes along their path, the thermohaline properties of their upper limb contributions are almost indistinguishable upon arrival in the NBC. Profiling floats and CTD sections (Ruscianno et al., 2012), as well as regional Lagrangian model analyses (Boebel et al., 2003; Rimaud et al., 2012), have shown that the Cape Basin plays a particularly important role in this context.

## 2.2. Tropics

As noted above, the main conduit for upper-limb AMOC transport across the equator is the NBC, which becomes organized as a western boundary current north of 10°S, fed by the SEC branches from the interior. South of 10°S, mean surface flow is mostly westward (Maximenko et al., 2009) as part of the subtropical gyre and the SEC. Any particle destined for the northward AMOC flow has to overcome southward Ekman transport induced by the trade winds. Indeed, surface trajectories simulated from the drifter-derived mean flow field by Lumpkin and Garzoli (2005) do not reach the equator unless they already start north of 10°S, pointing to the role that time-varying features such as eddies play for the AMOC here. Once north of the equator, particles experience the Coriolis force pulling them away from the coast, resulting in a retroflection into the North Equatorial Countercurrent (NECC). There is a strong seasonal cycle to the equatorial current system, with annual and semianual periodicity dominating the NECC and northern SEC, respectively (Lumpkin & Garzoli, 2005). Using a numerical model with nominally 1.4° resolution, Halliwell et al. (2003) conclude that particles in the NBC are most likely to proceed along the coast without being retroflected if they are inshore, shallow, and passing through the area at the right time of the year (late boreal winter and spring). Under these conditions, the boundary current can be a direct AMOC path into the Caribbean and subsequently the Florida Current. Other typical paths involve deflections into the interior ocean in the equatorial region (Fratantoni et al., 2000; Halliwell et al., 2003). There, equatorial upwelling and atmospheric forcing cause water mass transformation, and the seasonal equatorial currents lead to convoluted pathways (especially the NECC and the Equatorial Undercurrent). Some water particles will track all the way from the American to the African coast. Figure 3b shows observed surface drifter trajectories with NBC, NECC, Caribbean, and interior pathways.

Additional observed trajectories along some of these pathways and especially those of the rings shed by the NBC retroflection area are given by Fratantoni and Richardson (2006). North of the equatorial region, the trade wind induces northward Ekman drift that now aligns with the upper-limb AMOC flow, and water particles that have managed to escape the equator to the north in the open ocean will tend to be picked up by this and the westward North Equatorial Current. This, too, will lead to the Caribbean and ultimately the Gulf Stream. Transit times through these interior paths are reportedly 2–4 years, whereas the direct

boundary route from the southern hemisphere to the Gulf Stream takes less than 1 year (Halliwell et al., 2003).

The deeper parts of the upper AMOC limb, accounting for water depths below the thermocline to about 1,000 m, are occupied by Antarctic Intermediate Water (AAIW). The AAIW interior and western boundary pathways into the tropics have been documented by Boebel et al. (1999, 2003). AAIW too is subject to a zonally aligned equatorial current system of distinct seasonality (Ollitrault et al., 2006), which is different in shape and temporal evolution from that at the surface but poses a similar challenge for water particles to cross. Emerging north of the equator through interior pathways or the North Brazil Undercurrent (Lankhorst et al., 2009), the tracer signature of AAIW eventually fades out at the northern edge of the tropics as it encounters Mediterranean Water head-on (Sévellec et al., 2017), as well as subtropical Central Water from above and NADW from below.

### 2.3. North Atlantic Subtropics

The AMOC pathways from the tropics into the subtropical North Atlantic are mainly routed through the Caribbean Sea, as evidenced from a comprehensive analysis of surface drifters over the past several decades (Fratantoni, 2001; Lumpkin & Johnson, 2013). Exiting the Caribbean through the Yucatan Channel and into the Gulf of Mexico, the waters in the upper limb form part of the highly energetic and variable Loop Current before they are exported through the Florida Straits (Figure 3a). In agreement with these pathways deduced from surface drifters, Schmitz and McCartney (1993) show that the T-S signature on density surfaces in the Straits of Florida more closely resembles the T-S signature found south of the equator than in the North Atlantic subtropical gyre. The tropical origin for these waters has also been confirmed with a nutrient analysis (Palter & Lozier, 2008). Early hydrographic studies estimated that ~45% of the transport through the Florida Straits could be attributed to waters from the Southern Hemisphere (Schmitz et al., 1993; Schmitz & McCartney, 1993). This AMOC estimate (13 Sv) for the imported waters is lower than the AMOC mean (~17 Sv) at 26.5°N (Baringer et al., 2018; McCarthy et al., 2015), suggesting a sizeable contribution to the AMOC at 26.5°N from waters east of Abaco.

The AMOC waters exiting the Florida Straits (i.e., the Florida Current) join recirculating waters from the southern limb of the North Atlantic subtropical gyre to form the Gulf Stream. Here, in addition to surface drifters, there are a number of subsurface floats that trace the path of the Gulf Stream northward toward Cape Hatteras and then eastward from that point. Early studies of SOFAR floats at 700 m (Owens, 1991; Richardson, 1992) revealed strong entrainment and detrainment along the Gulf Stream path, indicating that once the upper limb of the AMOC left the rather narrow confines of the Florida Straits, the waters of tropical origin were mixed with waters to the north and south of the Gulf Stream. Analyses of RAFOS floats deployed in the Gulf Stream off Cape Hatteras in the 1980s and 1990s for the express purpose of studying frontal processes (Bower & Rossby, 1989; Song et al., 1995) attributed such strong exchange to the presence of meanders and, to a lesser extent, to the formation and expulsion of Gulf Stream rings. A striking feature revealed by these RAFOS floats is that cross-frontal exchange increases with depth, a feature explained by both kinematic (Bower, 1991) and dynamic (Bower & Lozier, 1994; Lozier & Bercovici, 1992; Lozier & Riser, 1989) arguments.

These early Lagrangian views led to an understanding that the transit of the waters within the upper AMOC limb toward the subpolar gyre is heavily influenced by the dynamics of the subtropical gyre. Specifically, surface waters in the Gulf Stream are largely recirculated into the subtropical gyre, while Gulf Stream waters at depth bifurcate, with some waters recirculating to the south, yet others branching northward. An analysis of profiling floats released in the subtropical gyre from 1997 to 2002 (Kwon & Riser, 2005) yields a striking image (Figure 4) of the subsurface upper-limb pathways from the Gulf Stream to the subpolar gyre via the North Atlantic Current.

The question as to how waters of the upper limb are imported to the subtropical North Atlantic via surface currents, yet exported below the surface, is answered by considering the impact of buoyancy forcing over the subtropical gyre. The transformation of surface waters within and to the south of the Gulf Stream into Subtropical Mode Water (otherwise known as Eighteen Degree Water) via winter cooling has been known for decades (Worthington, 1958), but more recent studies have revealed that this transformation facilitates the export of the upper AMOC limb. As shown by Gary et al. (2014), simulated particles launched within

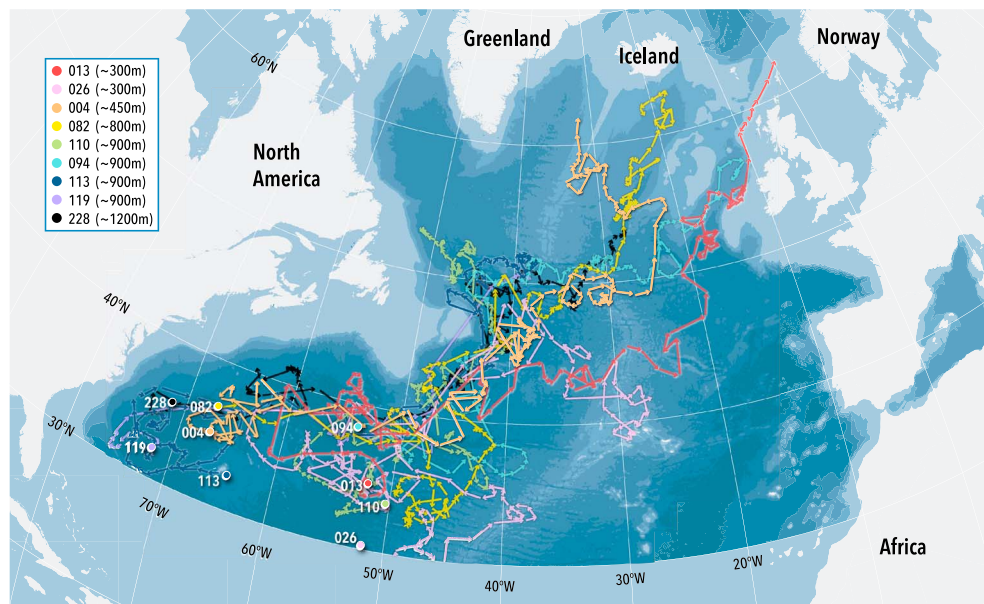


**Figure 4.** Trajectories of nine selected profiling floats that entered the subpolar gyre from the subtropics. The trajectory of each float is plotted with different color as specified in the legend, with dots indicating deployment positions and arrows indicating direction of travel. The legend also contains the approximate depth of each float. Since only the submerged displacement is plotted, the arrows are slightly disconnected. Bottom topography is shaded at 1,000-m intervals. The straight line over the Flemish Cap is not a real trajectory but is due to the failure of Float 119 to surface for 106 days. Figure adapted from Kwon and Riser (2005).

the Subtropical Mode Water circulate within the subtropical gyre but are eventually exported to the subpolar gyre. These export pathways have been confirmed by floats launched during the CLIMODE program (Fratantoni et al., 2013; The CLIMODE Group, 2009) for the purpose of studying the fate of the subtropical mode waters. Overall, the waters in the AMOC upper limb, subject to both the dynamics and thermodynamics of the subtropical gyre, leave the subtropical gyre with altered properties and spend longer in the gyre than would be expected if they were simply advected to the subpolar gyre along the surface Gulf Stream path.

#### 2.4. North Atlantic Subtropical-Subpolar Intergyre

The roughly 15-Sv transport of thermocline waters from the subtropical gyre to the subpolar gyre is a major contributor to the global midlatitude meridional heat transport (Trenberth & Fasullo, 2017; Willis, 2010) and supplies nutrients to the high-latitude North Atlantic (Palter & Lozier, 2008). Lagrangian studies have improved our understanding of this intergyre connection, its variability, and the origin/fate of the waters that connect across this strong frontal region.

This intergyre connection seems apparent at the surface from a quasi-Eulerian perspective of the large-scale circulation calculated from surface drifter velocities (Fratantoni, 2001), yet only one of the 273 drifters deployed south of 45°N between 1990 and 2002 connected across the gyre boundary (Brambilla & Talley, 2006). This surface exchange increased after 2002, but only to a maximum of 3.3% (Häkkinen & Rhines, 2009), far less than would have been inferred from the quasi-Eulerian view. Thus, surface drifter trajectories have shown that there is actually very little intergyre connectivity at the surface.

Lagrangian studies have suggested that the upper limb connection is instead provided by the gradual northward shoaling of isopycnals along the Gulf Stream-North Atlantic Current path. This connection is seen in profiling floats (Kwon & Riser, 2005) and Lagrangian modeling studies (Burkholder & Lozier, 2011b; Foukal & Lozier, 2016; Gary et al., 2014; Häkkinen et al., 2011; Kwon et al., 2015). Though more often connected to the supply of subtropical mode water to the subpolar latitudes, this latter mechanism also advects highly saline Mediterranean overflow waters into the Rockall Trough along the eastern boundary (Bower et al., 2002; Burkholder & Lozier, 2011a; Lozier & Stewart, 2008).

Modeling studies also allow for the calculation of trajectories backward in time to determine the source region(s) of high-latitude waters. These studies have suggested that the majority (65-80%, or upward of 17

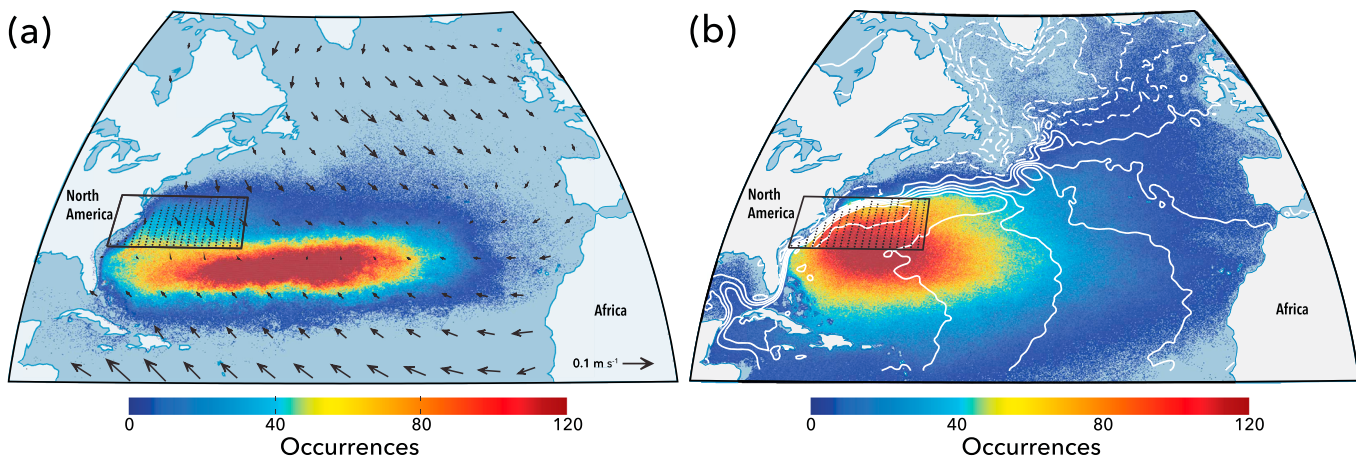


**Figure 5.** Distribution of modeled Gulf Stream waters. Fluid particle trajectories are initialized at the surface in the black box and integrated for 5 years in the 1/12° FLAME model through either the (a) two-dimensional surface velocity field or (b) three-dimensional flow field. The colors refer to the number of times a particle passed through a given location over the 15-year model run. Less than 0.01% of the trajectories reach the subpolar gyre when restricted to the surface velocity field (a) and only 2.51% reach the subpolar gyre when allowed to follow the three-dimensional flow field (b) after 5 years. These results demonstrate the lack of a direct connection between the surface Gulf Stream and the subpolar gyre. Arrows in (a) indicate the time-averaged Ekman velocities over the North Atlantic, showing a convergence zone at 30°N. Contours in (b) indicate the time-averaged SSH field over the North Atlantic, with positive values in solid contours and negative values in dashed contours. Figure adapted from Foukal and Lozier (2016).

Sv of transport) of the upper thermocline waters in the eastern subpolar gyre originate in the subtropics with the rest largely coming from the western subpolar gyre (Figure 5; Desbruyères et al., 2013; Burkholder & Lozier, 2014; Foukal & Lozier, 2018). Furthermore, the variability in the inter-gyre connection has been shown to be a strong contributor to the ocean heat content variability of the eastern subpolar gyre (Desbruyères et al., 2015; Foukal & Lozier, 2018).

## 2.5. North Atlantic Subpolar to Nordic Seas

The continued northward progression of relatively warm waters of subtropical origin is confined to the eastern subpolar north Atlantic. Quasi-Eulerian analyses of surface drifter velocities such as in Fratantoni (2001) show the strongest mean advective pathways through the Iceland Basin and Rockall Trough, where peak mean speeds reach 21 and 28 cm/s, respectively, and eddy kinetic energy levels are maximum for the subpolar region. These two branches of the NAC are evident in all surface drifter-based circulation studies of this region. More recent analyses of hydrographic data put the total northward upper limb AMOC transport associated with the NAC at 16–20 Sv, with about 90% of this total located in the Iceland Basin (Daniault et al., 2016; Mercier et al., 2015; Sarafanov et al., 2012). This indicates that the Iceland Basin, and not the Rockall Trough, is the primary conduit for the northward flux of warm waters.

Continuation of these pathways into the Nordic Seas, where waters are further transformed into the densest water masses of the North Atlantic (NADW), is more evident in some quasi-Eulerian maps of mean surface velocity derived from drifters than others, a result of low data density around and over the Greenland-Scotland Ridge, the shallow bathymetric feature that separates the subpolar North Atlantic from the Nordic Seas. For example, Fratantoni (2001) and McClean et al. (2002) show an abrupt deceleration and discontinuation of these branches at the ridge, while Orvik and Niiler (2002), Jakobsen et al. (2003), Rønnegaard, 2004; Figure 6), and Marsh et al. (2017) all show evidence of continuous mean flow over the ridge, probably due to the inclusion of more regional drifter trajectories in the latter analyses.

Not all the water that is eventually transformed into NADW originates from the near-surface layer of the subpolar region. Bower et al. (2002) released more than 100 isopycnal, acoustically tracked floats in the North Atlantic Current where it crosses the mid-Atlantic ridge in order to quantify subsurface (thermocline) pathways of the AMOC upper limb. Consistent with the transport estimates described above, these floats show a dominance of the NAC branch in the Iceland Basin compared to that in the Rockall Trough. But continuation of the trajectories northward over the Greenland-Scotland Ridge into the Nordic Seas was not observed with these floats for several reasons: (1) many floats recirculated in the subpolar gyre and thus

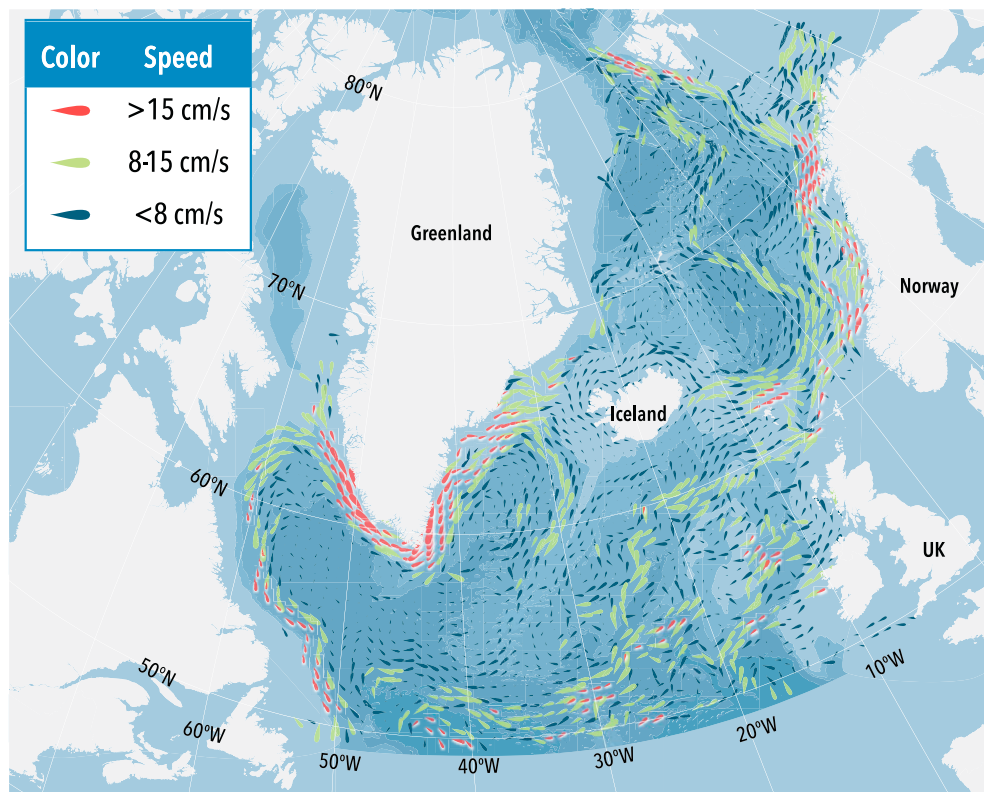


**Figure 6.** Quasi-Eulerian current vectors derived from 18-day low-passed filtered surface drifter trajectories and averaged in overlapping 1° latitude × 2° longitude boxes. Bottom topography is shaded at 1,000-m intervals. Figure adapted from Ribergaard (2004).

never reached the ridge, (2) many of the float trajectories were too short to make it to the ridge at the head of the Iceland Basin, and (3) those that did were on slightly deeper isopycnals, making it physically impossible to cross over the shallow ridge. This latter issue was addressed directly by Rossby et al. (2009) using 22 acoustically tracked floats released in the Iceland Basin just south of the Iceland-Faroes Ridge at ~200 m. These floats drifted into the Norwegian Sea over deep channels west and east of the Faroes Islands, consistent with transport estimates from vessel-mounted ADCP (Rossby et al., 2018).

The branches of the relatively warm water flowing over the Iceland-Scotland Ridge continue northward west of Norway. Poulain et al. (1996) analyzed the tracks of 107 surface drifters released throughout the Nordic Seas during 1991–1993 to provide the first basin-scale maps of the near-surface circulation from in situ observations. They describe two branches of the Norwegian Atlantic Current (NWAC) and the Norwegian Coastal Current (NWCC). The eastern branch of the NWAC and the NWCC merges and accelerates to instantaneous speeds greater than 110 cm/s west of the Lofoten and Vesterålen Islands (68°N). Combining this drifter data set with many more recent drifter trajectories, Andersson et al. (2011) provide more detail on the structure and variability (on seasonal to decadal time scales) of the NWAC and NWCC, and particle diffusivities. They show elevated EKE along the path of the NWAC, whose mean currents are about 20% stronger in winter. Clustering of the data according to bottom depth before averaging lends better resolution of the various current branches as well as the spatial structure of particle diffusivity (Koszalka et al., 2011).

As illustrated by the recirculating subsurface floats in Bower et al. (2002), and the numerous surface drifter studies cited above, a totally separate branch of the upper limb of the AMOC circulates cyclonically around the subpolar region as part of the wind-driven subpolar gyre, with its waters continually cooling and ultimately forming the intermediate-depth Labrador Sea Water (LSW), the lightest component of NADW. Daniault et al. (2016) estimate 6.4 Sv of remnant NAC waters crossing the Reykjanes Ridge from east to west. In the near-surface layer, analyses of surface drifter data indicate that the mean current speed along this circuitous boundary-following path is highly variable, with slower mean currents in the northern ends of all three subbasins, and east of the Reykjanes Ridge (Cuny et al., 2002; Flatau et al., 2003; Fratantoni, 2001).

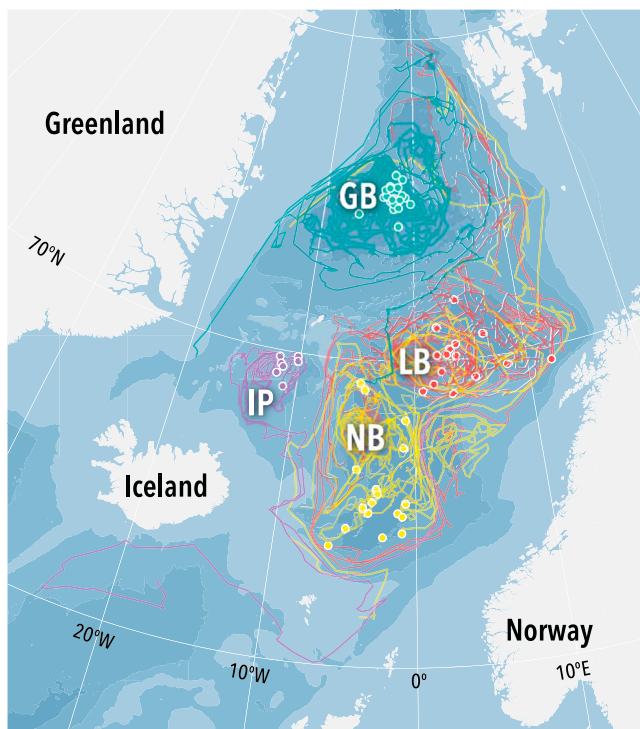


**Figure 7.** Circulation within the four major basins of the Nordic Seas. Four groups of profiling floats deployed inside the shallowest closed contour of each of the following: the Greenland Basin (labeled “GB”; green-blue trajectories), Lofoten Basin (LB; red), Norwegian Basin (NB, yellow), and Iceland Plateau (IP, purple). Launch locations are denoted by dots, and trajectories are of unequal duration. Deployments took place between 2001 and 2008, and drift depth was  $\sim 1,000$  m. Bottom topography is shaded at 1,000-m intervals. Figure adapted from Voet et al. (2010).

While mean speeds in the interior may be less than along the boundaries, Lagrangian observations reveal “hot spots” of mesoscale eddy activity, including long-lived coherent vortices, in the Iceland Basin and Rockall Trough, west of the Reykjanes Ridge, and west of Greenland (Bower et al., 2002; Fratantoni, 2001; Prater, 2002; Shoosmith et al., 2005).

### 3. AMOC Lower Limb

Compared to the surface ocean, where thousands of drifter trajectories are available to map out the pathways of the AMOC’s upper limb with some statistical confidence, identifying all the pathways of the southward return flow of cold dense water from a Lagrangian perspective is more challenging due to an order of magnitude fewer subsurface float trajectories. As a result, in some regions of the deep Atlantic Ocean, such as the SA, the Lagrangian view is at this time almost entirely informed by the analysis of simulated particle trajectories.

#### 3.1. Nordic Seas

The densest water masses transported southward through the Atlantic by the deep limb of the AMOC, constituting Lower NADW (LNADW), emerge from the Nordic Seas as dense overflows across the Greenland-Scotland Ridge. Long-term mean estimates of overflow transports (potential densities greater than 27.8) at the sill are 3.0–3.5 Sv of Denmark Strait Overflow Water (DSOW) between Greenland and Iceland, 1.0 Sv between Iceland and the Faroe Islands, and about 2.0 Sv of Iceland-Scotland Overflow Water (ISOW) south of the Faroe Islands (Dickson et al., 2008). In the last 10 years, there has been an increasing interest in the pathways of the dense waters as they make their way to these restricted outlets from the Nordic Seas since water parcel routes and residence times impact the properties (temperature, salinity, and density) of the water entering the general circulation of the global ocean. In one of the first observational subsurface Lagrangian studies in the Nordic Seas, Søiland et al. (2008)

released 22 acoustically tracked floats at 800 m over the northern slope of the Iceland-Faroe Ridge and found that the source of the dense overflow through the Faroe Bank Channel at the time of the observations was from the west, and not from the interior Norwegian Sea, although the latter path may be favored under different wind forcing conditions (Köhl, 2010). Some of the 52 deep floats deployed farther west in the Iceland Sea by de Jong et al. (2018) show a path southeastward with the East Icelandic Current and then, for two floats, along the northern slope of the Iceland-Faroe Ridge toward a probable escape through the Faroe Bank Channel.

Other floats in the de Jong et al. (2018) study reveal a dominance of the East Greenland Current, compared to the North Icelandic Jet (NIJ; Jonsson & Valdimarsson, 2004; Våge et al., 2011), as the primary source of the dense overflow through Denmark Strait. The authors argue that this may be the result of “NIJ-unfavorable” wind stress curl over the Iceland Sea during the float observational period.

In a larger-scale Lagrangian study of the circulation within the Nordic Seas, Voet et al. (2010) analyzed observations from about 60 profiling floats released throughout the Greenland, Iceland, and Norwegian Seas, with drifting depths of  $\sim 1,000$  m (Figure 7). They found that the circulation pattern is strongly constrained by topography. The deep flow is cyclonic, both on the large scale and within individual basins, with the internal gyres having transports of  $\sim 15$  Sv, that is, about 3 times larger than the dense overflow transport into the North Atlantic.

Two numerical model studies use simulated particle trajectories to investigate the pathways of the deep waters feeding the dense overflows. Köhl (2010), using the MIT/GCM, found that pathways to the overflows depend strongly on wind forcing patterns. For example, strong wind stress curl led to a dominance of the East Greenland Current over the NIJ as the feeder source for DSOW, consistent with the observations of

de Jong et al. (2018). Behrens et al. (2017) simulated particle motion in the Iceland Sea using the high-resolution VIKING20 model and also associate variability in deep pathways to interannual wind stress curl changes. Using simulated particle trajectories, they were also able to identify the overturning loop north of Iceland that has been hypothesized to feed the NIJ (Våge et al., 2011).

### 3.2. Subpolar North Atlantic

Lagrangian observations of the descent of the dense overflows of DSOW and ISOW into the subpolar North Atlantic are technically difficult and have not yet been realized in significant numbers of trajectories, although notably Prater and Rossby (2005) successfully followed the ISOW plume in the Iceland Basin with several bottom following floats. However, two studies use simulated particle trajectories derived from a high-resolution configuration of the MITgcm to investigate the pathways and evolution of the descending DSOW. Koszalka et al. (2013) estimated transit times from the sill to  $\sim 63^{\circ}\text{N}$  at 2-3 weeks and used reverse particle tracking to show that at this downstream location, about 25% of the particles in the overflow plume are not coming from the sill itself but are dense waters from the East Greenland shelf that have spilled over the shelf break at upstream locations. von Appen et al. (2014) also use reverse particle tracking in the same model to argue that there are actually three sources to the so-called Spill Jet (Pickart et al., 2005): the shelf and sill in Denmark Strait, and entrained Irminger Current water from the Irminger Sea.

A number of recent studies review NADW (including LNADW and LSW/UNADW, the latter formed by open ocean deep convection in the western subpolar gyre) transport estimates at various locations around the subpolar region, based mostly on current meter observations (Daniault et al., 2016; Kanzow & Zenk, 2014; Zantopp et al., 2017). Lagrangian observations in the deep subpolar North Atlantic are more rare and until recently were confined mainly to the LSW level. The analysis of 89 acoustically tracked floats released in the Iceland Basin mostly at the LSW level by Lankhorst and Zenk (2006) revealed relatively strong flows southwestward along the eastern flank of the Reykjanes Ridge, with the possibility of westward escape from the Iceland Basin through deeper gaps in the ridge, including the Bight Fracture Zone. Funk et al. (2009) analyzed trajectories of 12 acoustically tracked floats released in the central Labrador Sea specifically to determine how quickly LSW from the interior enters the boundary current. They found a maximum in eddy diffusivity in the interior region and concluded that this contributed to rapid homogenization of newly formed LSW in the interior, followed by a slower entrainment into the boundary current.

LNADW pathways in the subpolar North Atlantic are presently being investigated in detail as part of the on-going international Overturning in the Subpolar North Atlantic Program (OSNAP; Lozier et al., 2017). Since 2014, about 120 acoustically tracked floats have been deployed in the depth range 1,800-2,800 m in the deep boundary current of the subpolar North Atlantic at various sites to identify regions of enhanced boundary-interior exchange, and better define dominant spreading pathways and their low-frequency variability. Preliminary results have revealed the importance of ISOW pathways from the Iceland to Irminger Basins through gaps in the Reykjanes Ridge (as also found by Lankhorst & Zenk, 2006, for LSW), the lack of an ISOW pathway into the Irminger Basin from the Charlie-Gibbs Fracture Zone, and the prevalence of deep cyclonic eddies in the DSOW plume around southern Greenland (Bower et al., 2017).

Some early float trajectories from OSNAP were combined with simulated particle trajectories and current meter observations by Zou et al. (2017) to investigate the export pathways of ISOW from the Iceland Basin. From the simulated trajectories, they found that after 10 years,  $\sim 20\%$  of ISOW had escaped into the Irminger Sea via gaps in the Reykjanes Ridge, including the Charlie-Gibbs Fracture Zone; 20% was exported due south into the West European Basin; and the remainder was still recirculating within the Iceland Basin. These results highlight the potential importance of a previously underappreciated southward ISOW pathway entirely in the eastern basin. Lankhorst and Zenk (2006) reported one RAFOS float that flowed southward at  $\sim 2,700$  m (ISOW level) along the eastern flank of the MAR until  $48^{\circ}\text{N}$ , and several OSNAP floats at the ISOW level follow a similar path (Bower et al., 2017). Simulated trajectories calculated for 10 years follow a similar path into the West European Basin as far south as  $43^{\circ}\text{N}$ . Interestingly, when heading southward, ISOW takes both boundary current (along the eastern flank of the MAR) and interior pathways. Zou et al. (2017) also found that the strength of the export pathways westward through the CGFZ and southward along the eastern flank of the mid-Atlantic ridge were anticorrelated on interannual time scales. This is one of only a few studies investigating interannual variability in AMOC pathways.

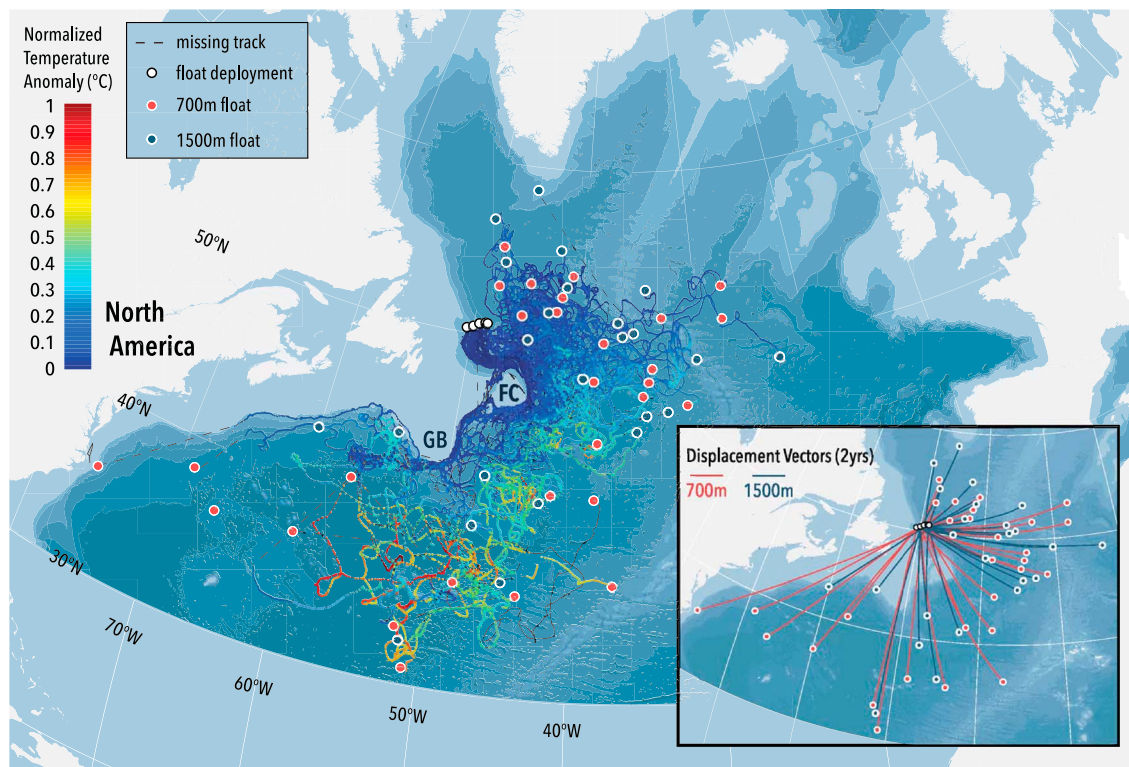


**Figure 8.** Two-year trajectories of 53 acoustically tracked RAFOS floats released at 700 and 1,500 m in the Deep Western Boundary Current near 50°N. Colors indicate the normalized temperature anomaly, defined as  $(T - T_i)/\delta T_{\max}$ .  $T_i$  is each float's initial temperature, and  $\delta T_{\max}$  is the maximum temperature range observed by the floats as a group, 6.4°C at 700 dbar and 1.8°C at 1,500 dbar. The dashed lines indicate missing track. The inset shows the 2-year displacement vectors for the same floats. Bottom topography is shaded at 1,000-m intervals. Adapted from Bower et al. (2013).

### 3.3. North Atlantic Subpolar-Subtropical Intergyre

Until relatively recently, the DWBC was assumed to be the major conduit for the lower limb of the AMOC at all latitudes in the Atlantic, including at the North Atlantic subpolar/subtropical gyre boundary. This idea was first introduced theoretically by the seminal work of Stommel and Arons (1960a, 1960b) using a first-order vorticity balance. Its existence was first confirmed with some of the earliest subsurface float trajectories (Swallow & Worthington, 1957), and later studied in more detail by observations that revealed deep water transport and property cores along the western boundary in the North Atlantic (e.g. Smethie et al., 2000; Talley & McCartney, 1982; Toole et al., 2017). Direct observations within the DWBC near the gyre boundary (43°N) revealed a NADW “export” (below 27.74 kg/m<sup>3</sup>) of 12.2–15Sv (Schott et al., 2004, 2006). However, without basin-spanning measurements of the deep waters, it is not clear what fraction of this deep transport is recirculated. Emerging Lagrangian studies have brought valuable insights to this knowledge gap.

An analysis of profiling floats released in the subpolar North Atlantic (Lavender et al., 2000) found that none of the floats at 1,500 m (a typical LSW level) were able to pass south of the Flemish Cap (48°N) via the DWBC. Instead, the floats drifted offshore to the basin interior by eddy-driven cross-isobath flow. Similar conclusions were made by Fischer and Schott (2002) with 15 profiling floats released purposely in the DWBC at 53°N. Concerns were raised that the profiling floats did not stay within the DWBC because their release was too near strong recirculations and/or because when the floats periodically surfaced for position fixes, the upper-ocean currents deflected them from their equatorward pathways along the western boundary. These concerns were addressed by Bower et al. (2009, 2011), who tracked LSW pathways with subsurface RAFOS floats released in the DWBC at the exit of the subpolar gyre (~50°N). A large fraction of floats (70%) were deflected off the boundary, drifting eastward along the path of the deep NAC (Figure 8). Most of the southward drifting floats that passed Flemish Cap were also deflected from the

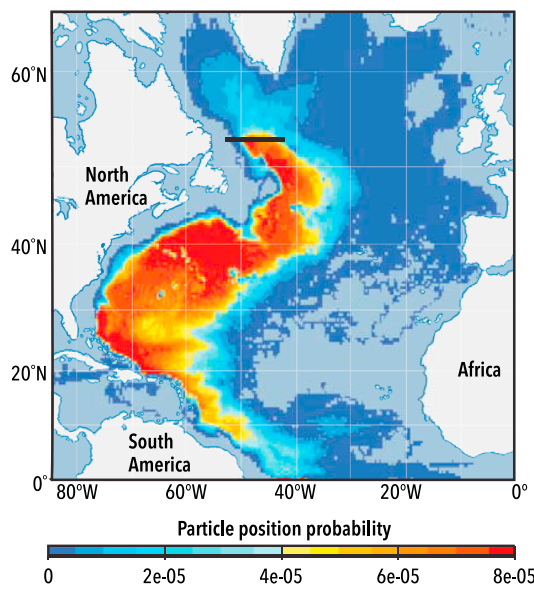


**Figure 9.** Probability map of Overflow Water (i.e. the Lower North Atlantic Deep Water,  $<2.3^{\circ}\text{C}$ ) particles launched at  $53^{\circ}\text{N}$  from  $\sim 2,500$  to  $4,000$ -m depth within the Deep Western Boundary Current (black line) over the course of 50 years. Adapted from Lozier et al. (2013).

travels westward above/through the MAR to the western basin where it is exported. It is also possible that it is not exported to the subtropics at all but instead participates in an eastern-basin-only overturning (Van Aken, 2000).

The interior pathways revealed by observed and simulated particle trajectories highlight the significant exchange between the DWBC and basin interior at the latitudes of the subpolar-subtropical transition, which has been attributed to the presence of coherent eddies and other mesoscale processes (e.g. stirring and mixing) in the deep layer (Bower et al., 2013; Gary et al., 2011; Lozier, 1999), and the presence of eddy-driven mean recirculation (Lozier, 1997). They further imply that measuring DWBC transport alone, albeit important, does not capture the total export in the AMOC lower limb. The same holds for efforts to capture export variability. It is interesting to note that simulated particle trajectories, when released in abundance, are able to capture the spreading passive tracer export, hence are able to follow and represent the spreading of CFC and anthropogenic  $\text{CO}_2$  (Gary et al., 2012).

### 3.4. North Atlantic Subtropics

Notwithstanding uncertainties in the fate of ISOW in the eastern North Atlantic, the primary pathway of the lower limb of the AMOC through the subtropics begins with the DWBC at the Grand Banks. As discussed in the last section, a portion of the NADW transported by the DWBC is carried into the interior from several sites along the boundary around the Grand Banks (e.g., Bower et al., 2009, 2011; Rhein et al., 2002). Fifty-year simulated particle trajectories show that this water spreads and fills the subtropical region west of the MAR to about  $37^{\circ}\text{N}$  (Gary et al., 2011), with a portion of the transport of LSW apparently accomplished by coherent eddies (Bower et al., 2013).

Once past the Grand Banks, the remaining and/or modified NADW transported by the DWBC continues along the western boundary relatively undisturbed (Bower & Hunt, 2000a), until it reaches Cape Hatteras. The 10-year mean transport of the DWBC just upstream of Cape Hatteras ( $39^{\circ}\text{N}$ ) has been estimated to be 18.4–22.8 Sv at “Line W,” depending on whether the lightest LSW was included (Toole et al., 2017). As described in previous sections, without accompanying transbasin transport estimates, it is not certain what fraction of this transport is locally recirculated versus exported southward.

To continue southward, the DWBC must cross under the Gulf Stream. Bower and Hunt showed directly with 800-m RAFOS floats that the upper portion of the DWBC is redirected offshore following contours

boundary and entered the subtropical gyre via interior pathways (17%), with less than 10% of the floats following the DWBC continuously around the Grand Banks. At least some of the LSW transport into the interior appears to be accomplished via coherent vortices spun off the slope of the Grand Banks (Bower et al., 2013). Model-based Lagrangian simulations, with extended spatial and temporal domain, further confirmed the importance of these interior pathways in exporting LSW to the subtropical gyre (Getzlaff et al., 2006; Bower et al. (2009, 2011); Zou & Lozier, 2016).

In the absence of Lagrangian observations, the southward export of LNADW to the subtropics has been mostly studied with simulated particle trajectories. Lozier et al. (2013) tracked LNADW with simulated trajectories in the western North Atlantic using output from an ocean general circulation model and found that in addition to the DWBC, interior pathways carry significant amounts of LNADW to the subtropical gyre (Figure 9). They further pointed out that, in contrast to LSW export, LNADW export is primarily equatorward, with limited recirculation within the subpolar gyre (also in Gary et al., 2011). The equatorward transport of ISOW is also implicated in the eastern subpolar North Atlantic (see previous section). However, whether and how ISOW following this path is exported to the subtropical gyre is still unclear. Further study is needed to ascertain whether it is exported via continued southward spreading in the eastern North Atlantic or tra-

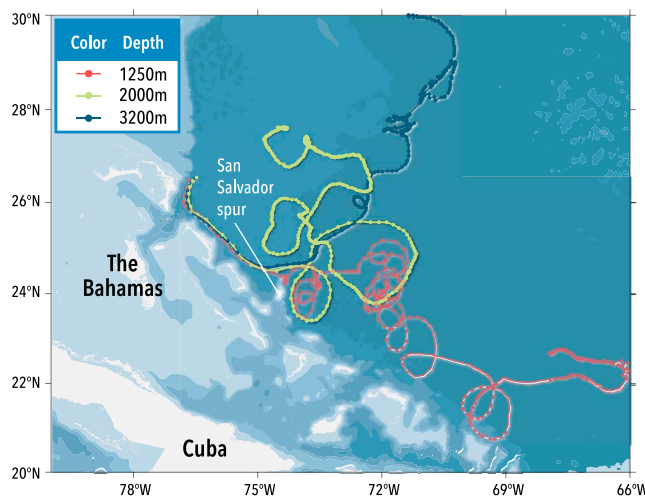


**Figure 10.** Floats at three depths, deployed simultaneously, first drift in Deep Western Boundary Current along the continental slope, and then are deflected offshore at the San Salvador Spur. Bottom topography is shaded at 1,000-m intervals. Adapted from Leaman and Vertes (1996).

30°N. Transport measured at 26.5°N, along the “Abaco line,” equivalently measured as at Line W was 13.9 Sv (Toole et al., 2017). Toole et al. (2017) state that the decrease in mean transport may be due to the recirculation present at Line W compared to downstream, and this is reflected by the float pathways between the two mooring arrays. One float at 3,000-m depth drifted continuously equatorward along the western boundary in the DWBC from 43 to 21°N in 2 years (Bower & Hunt, 2000a). This time scale is one direct measure of what is probably the minimum, or fastest, transit time through the subtropics, based on the directness of the pathway and the typical DWBC speed of the float (Bower & Hunt, 2000a).

In an earlier experiment by Leaman and Vertes (1996), floats launched at 26°N in the DWBC generally drifted continuously along the boundary until they reached the San Salvador Spur at about 24°N, where some floats at 1,250, 2,000, and 3,000 m were deflected off the boundary, depending on the proximity of the DWBC core to the Spur (Figure 10). Model results (Xu et al., 2012) also show recirculation patterns of the DWBC consistent with this view: in the mean, water is transported off the boundary at this location. Some of the floats become trapped in coherent eddies (of both polarities) that form at this location (Leaman & Vertes, 1996), with one anticyclone measured for 6 months.

### 3.5. Tropics

Simulated trajectories in the NADW (Gary et al., 2011) suggest that the lower limb of the AMOC is well confined to the DWBC as it enters the tropics from the north. This is different from interior pathways seen in the subtropical and subpolar North Atlantic (see above sections). The passages between the Antilles islands are generally too shallow to allow deep water through, leaving only the main basins of the tropical Atlantic as possible conduits. Localized narrow recirculations of the DWBC have been observed (Lankhorst et al., 2009; Richardson & Fratantoni, 1999; Richardson & Schmitz, 1993), but the DWBC continues to be the dominating feature of the southward AMOC east of the Caribbean, and southward along South America, until it reaches the equator. There, float observations show both a direct pathway along the western boundary, as well as large detours into the eastern Atlantic basin via zonal equatorial flows, much like what the upper waters experience on their northward journey. Richardson and Fratantoni (1999) report transit times of about a year to cross from 5°N to 5°S directly in the DWBC, with interior excursions lasting up to 4 years. Based on float velocities observed at 1,800-m depth, they report a southward volume transport of some  $6,000 \text{ m}^2/\text{s}$  per unit depth of layer thickness, which amounts to 21 Sv assuming a 3,500-m layer. This is consistent with transports observed by the MOVE mooring array at 16°N (Send et al., 2011). About twice as much actually flows southward in the DWBC but is partially compensated by recirculations and interior flow. South of the equatorial region, Dengler et al. (2004) report that the DWBC becomes unstable near

of lower layer potential vorticity and becomes part of the deep Gulf Stream and Northern Recirculation Gyre. One 800-m DWBC float did cross the Gulf Stream in a cold-core eddy formation event, but this was not the norm.

Deep (3,000-m) floats released at the NADW level in the DWBC either continued southward directly along the boundary at the Gulf Stream crossover or were diverted offshore (Bower & Hunt, 2000a, 2000b), and turned southward into the interior after the eastward diversion. The deep float pathways, including the bifurcation, can be explained in terms of deep potential vorticity distribution. Lower-layer PV between the descending thermocline of the Gulf Stream above and the seafloor dictated the path of travel of each float. Floats that reached the crossover region further west tended to cross more directly under the stream, while floats that hit the stream farther east exhibited more eddy motion and were more likely to be diverted eastward along an interior path paralleling the Gulf Stream. Both routes conserve lower-layer potential vorticity.

South of the crossover region, most floats were observed to travel more smoothly southward along the boundary, one float to 21°N. Some deep floats detached from the boundary as they passed the Blake Spur at

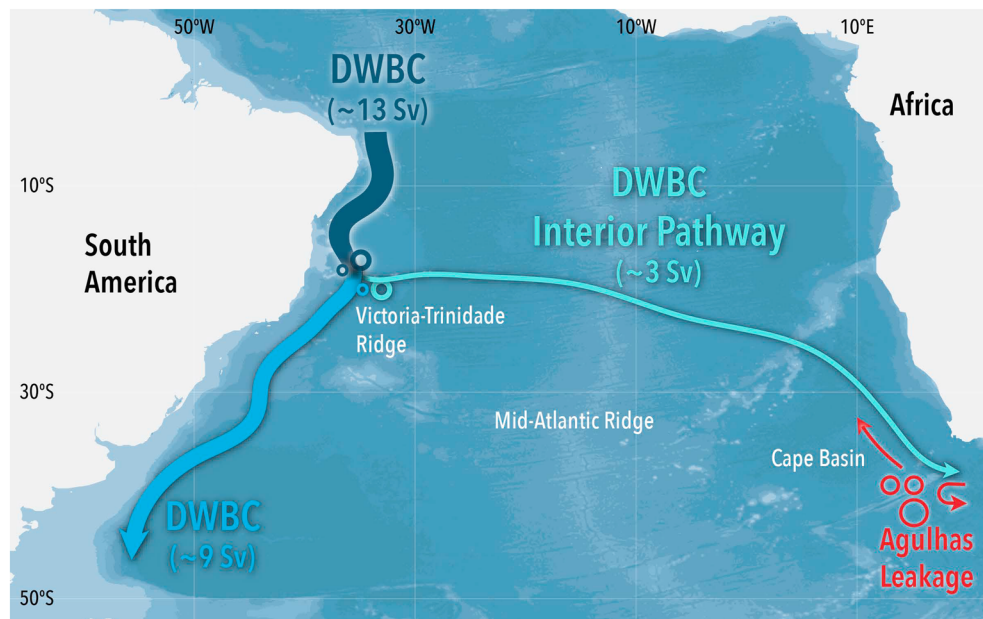


**Figure 11.** Schematic of North Atlantic Deep Water pathways in the South Atlantic as described by van Sebille et al. (2012) and Garzoli et al. (2015). The lower limb of the Atlantic Meridional Overturning Circulation (i.e. North Atlantic Deep Water) is shown in shades of blue, and some relevant pathways of the upper-limb Atlantic Meridional Overturning Circulation are shown in red. Bottom topography is shaded at 1,000-m intervals.

8°S and that continued southward AMOC flow occurs primarily via deep eddies that carry up to 25 Sv of volume transport. These eddies bear a strong resemblance and possibly share dynamics with the NBC rings discussed earlier.

### 3.6. South Atlantic

Simulated particle trajectories suggest that approximately  $13.2 \pm 3.1$  Sv of NADW form part of the AMOC lower limb and enter the SA basin across 5°S between 1,000-3,500m in depth (Garzoli et al., 2015; van Sebille et al., 2012). The primary pathway of NADW ( $9.4 \pm 4.2$  SV) follows the DWBC along the South American continental slope (Garzoli et al., 2015; Figure 11). A total of  $2.9 \pm 1.4$  Sv flows along the DWBC until the Vitória-Trindade Ridge, where it subsequently turns toward the basin interior and eventually joins the Cape Basin (Garzoli et al., 2015). While direct Lagrangian observations in this region are sparse, neutrally buoyant float trajectories confirm that the coherent pathway of the DWBC is interrupted by significant mesoscale activity around the Vitória-Trindade Ridge, which steers floats towards the interior (Hogg & Owens, 1999).

This zonal spreading of NADW following its detachment from the continental boundary, as well as its subsequent meridional (southeastward) motion in the Cape Basin, has been attributed to the existence of Agulhas rings (van Sebille et al., 2012). Firstly, as the rings migrate north-westward in the “Agulhas-eddy-corridor” across isolines of potential vorticity (PV), they indirectly induce the NADW’s compensating zonal flow *along* PV isolines. Secondly, as NADW reaches the Cape Basin, a divergent eddy-thickness-flux imposed by the rings, acts as an external forcing that depresses the NADW layer thickness, and triggers a meridional migration to conserve PV. This explanation is rather interesting, as it suggests that the behavior of NADW is intermittent and strongly influenced by the motion of the upper-limb AMOC (van Sebille et al., 2012). Finally, while modeling studies suggest that most NADW exits the SA across 45°S west of 45°W, they also suggest that a small fraction exits the basin near South Africa (~17°E) and that some recirculates in the basin for more than 300 years (Garzoli et al., 2015; van Sebille et al., 2012). This is also confirmed by the existence of NADW in the Cape Basin (Arhan et al., 2003) and further downstream in the Agulhas Undercurrent in the Indian Ocean off South Africa (Casal et al., 2006).

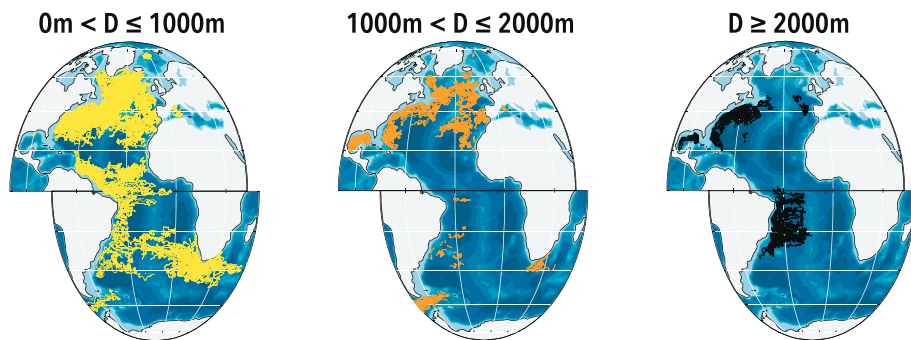


**Figure 12.** Subsurface float trajectories binned by depth, from left to right: 0–1,000 m; 1,000–2,000 m; and 2,000 m and deeper. Data source is the AOML PhOD subsurface drifter database, which currently houses all subsurface data collected through end of 2015 (Ramsey et al., 2018; [https://www.aoml.noaa.gov/phod/float\\_traj/](https://www.aoml.noaa.gov/phod/float_traj/)).

#### 4. Conclusions

In this review, we have collected Lagrangian studies, both observational and numerical, that focus on the pathways of the upper and lower limbs of the AMOC. A number of common themes emerge, which are also illustrated in Figure 1:

1. Recirculations and interior pathways: For both the upper and lower limbs of the AMOC, purely meridional pathways are disrupted by permanent recirculation cells or gyres where fluid parcels may reside for years or decades before moving on to the next latitudinal zone. This feature—entirely absent in conveyor belt images of the AMOC—has important implications for water mass transformation along the pathways of the AMOC, due to air-sea interaction and/or lateral stirring and mixing that occur within the recirculation cells. The most well-studied examples are the deep recirculations associated with the Gulf Stream and North Atlantic Current that direct a significant fraction of NADW along interior pathways of the North Atlantic subtropics. The existence of these recirculations and interior pathways also makes it challenging to observe AMOC transport and its variability from non-basin-crossing arrays since the measured transport may be inflated by local recirculations and/or completely miss interior transports. Recirculations may also delay and/or diminish the meridional propagation of climate change signals through the Atlantic. In Figure 1, we highlight locations along the AMOC boundary pathways where fluid particles have been observed to leave the boundary and move into the ocean interior. These “off-ramps” are more evident in the Lagrangian observations than the “on-ramps” because floats have been preferentially deployed in the boundary currents to identify exit points. Moreover, the pathways are usually of insufficient length to indicate the reentry locations. The recirculation arrows in Figure 1 should therefore not be interpreted as an along-path reduction in AMOC transport, but instead as reminders that the AMOC pathways are not pipes carrying the same fluid particles over long meridional distances. This is one of the most important contributions that Lagrangian observations and modeling studies have made to our understanding of AMOC structure.
2. Zonal pathways: In addition to the zonal flows associated with recirculations, there are several regions where AMOC pathways are more zonal than meridional. These seem to occur mostly at gyre boundaries and along the equator. Examples include the east-to-west path of the SEC in the SA, the west-to-east path of the North Atlantic Current at about 50°N, and the west-to-east path of NADW in the southern SA.
3. Lagrangian versus Eulerian views: There is no doubt that by binning velocity observations from large numbers of surface drifters or subsurface floats, we have gained new knowledge on the horizontal structure of the mean ocean circulation and eddy kinetic energy, especially at the sea surface. But through the analysis of the trajectories themselves, we have discovered how those quasi-Eulerian maps of mean velocity can sometimes be misleading when it comes to defining the three-dimensional structure of the AMOC. This has been illustrated here most clearly in the North Atlantic subtropical/subpolar intergyre region, where velocity maps from surface drifters show a smooth, continuous mean flow from the Gulf Stream to the North Atlantic Current and into the eastern subpolar gyre, but hardly any surface drifters follow that path. This apparent disconnect between Eulerian and Lagrangian views of the same data was

reconciled by considering the AMOC in density space, and recognizing that it is fluid parcels from the subtropical thermocline that connect most directly with the surface subpolar region. In this way, the truly Lagrangian (density-conserving) view aligns well with the density-based Eulerian view.

4. Eddies: Fluid particle trajectories, both observed and simulated, also indicate that mesoscale eddies, and not continuous boundary or interior currents, do the “heavy lifting” of the AMOC in some regions. This is most clearly demonstrated in two parts of the SA: in the east where Agulhas Rings transport warm water northward, and in the west, where the DWBC breaks up into coherent eddies that drift southward along the boundary. Other well-known examples are where the north Brazil Current retroflects and pinches off anticyclonic rings that drift northward toward the Caribbean, and in the Labrador Sea, where the remnants of the warm water carried northward and around the North Atlantic subpolar gyre spin off the boundary of west Greenland as anticyclonic eddies and drift into the interior, where they are transformed into LSW. Less well-documented but possibly important is the similar spin-off of LSW anticyclones around the Grand Banks. Lagrangian observations and simulations are particularly important for visualizing these features of the AMOC and assessing their impact on mass, heat, and freshwater fluxes.
5. Trajectory simulations: As the resolution and realism of ocean general circulation models continue to improve, fluid particle trajectory analyses based on model velocity fields will become an even more valuable tool for investigating the pathways of the AMOC. Simulated trajectories are computationally “cheap” compared to, for example, computing the evolution of a tracer field in a model (van Sebille et al., 2017) and have been shown, with sufficient number, to adequately capture the spread of tracers (Gary et al., 2012). Orders of magnitude more trajectories can be computed compared to the number that can be observed, and integrated out for years and even decades. There is also the ability to track fluid particles back in time, which is particularly useful for determining the origin of waters passing through a specific region. Furthermore, Lagrangian model output can be used to examine water mass transformations over long distances and investigate the structure of heat and fresh water fluxes along the AMOC pathways (e.g., Berglund et al., 2017; Chenillat et al., 2015; Durgadoo et al., 2017; Lique et al., 2010; Rimaud et al., 2012; Rühs et al., 2019; Speich et al., 2007). Of note is that simulated trajectories are perhaps least reliable in the deep ocean, where observations (Eulerian or Lagrangian) are too sparse to provide adequate model verification.

#### Acknowledgments

The authors extend their thanks to Xiaobiao Xu for valuable comments on the first draft of this manuscript. A. B. (WHOI), H. F., M. S. L., N. F., and K. D. were supported by Overturning in the Subpolar North Atlantic Program grants OCE-1259618, OCE-1259013, and OCE-1259102 from the U.S. National Science Foundation. S. Z. was supported by the Climate Program Office of the National Oceanic and Atmospheric Administration under award NA16OAR4310168. M. L. was supported through the MOVE project, funded by NOAA’s Global Ocean Monitoring and Observing Program under award NA15OAR4320071. A. B. (GEOMAR) and S. R. received funding from the Cluster of Excellence 80 “The Future Ocean” within the framework of the Excellence Initiative by the Deutsche Forschungsgemeinschaft (DFG) on behalf of the German federal and state governments (grant CP1412) and by the German Federal Ministry of Education and Research (BMBF) for the SPACES projects AGULHAS (grant 03F0750A) and CASISAC (grant 03F0796A). No new data are reported in this project. The data mentioned in the text may be found in repositories cited in each previously published paper cited in this review manuscript.

For the foreseeable future, Lagrangian observations will be required to resolve mesoscale aspects of the AMOC and its variability, especially in the subsurface ocean. Such observations are also needed to verify Lagrangian output from numerical models, as has been demonstrated in numerous studies (Bower et al., 2009; Bower et al., 2011; Burkholder & Lozier, 2011a, 2011b; Gary et al., 2011, 2012, 2014). There are still vast areas of the Atlantic that have not been observed in the Lagrangian frame. This applies to most of the depths occupied by the deep limb of the AMOC, especially in the SA, where there has been only one deep float study (Brazil Basin). Figure 12 shows all the available acoustically tracked subsurface float trajectories in the Atlantic, color-coded by depth (see Ramsey et al., 2018, for more details of the data distribution, an extension to the global view). The deep eastern North Atlantic, where recent studies suggest that a sizeable southward export of NADW may occur, perhaps as part of an eastern-basin-only overturning circulation, is another region that deserves more attention.

The growing deep Argo program may eventually help fill this gap, but it will take many years to accumulate sufficient data density to construct meaningful maps of the mean deep circulation. Additionally, these floats will likely undersample the continental slopes where major branches of the AMOC are found. Basin or sub-basin releases of deep acoustically tracked floats would provide this information more quickly. Installation of basin-scale acoustic positioning networks (Howe et al., 2019, manuscript in review), combined with development of a less expensive acoustically tracked float (T. Rossby, personal communication, July 2019), would facilitate a major leap forward in our knowledge of the deep ocean circulation, including the AMOC.

#### References

Andersson, M., Orvik, K. A., LaCasce, J. H., Koszalka, I., & Mauritzen, C. (2011). Variability of the Norwegian Atlantic Current and associated eddy field from surface drifters. *Journal of Geophysical Research*, 116, C08032. <https://doi.org/10.1029/2011JC007078>

Arhan, M., Mercier, H., & Park, Y.-H. (2003). On the deep water circulation of the eastern South Atlantic Ocean. *Deep Sea Research Part I*, 50(7), 889–916. [https://doi.org/10.1016/S0967-0637\(03\)00072-4](https://doi.org/10.1016/S0967-0637(03)00072-4)

Baringer, M., Willis, J., Smeed, D. A., Moat, B., Dong, S., Hobbs, W. R., et al. (2018). Meridional overturning and oceanic heat transport circulation observations in the North Atlantic Ocean. *Bulletin of the American Meteorological Society*, 99(8), S91–S94.

Beal, L. M., De Ruijter, W. P., Biastoch, A., Zahn, R., Cronin, M., Hermes, J., et al. (2011). On the role of the Agulhas system in ocean circulation and climate. *Nature*, 472(7344), 429.

Behrens, E., Väge, K., Harden, B., Biastoch, A., & Böning, C. W. (2017). Composition and variability of the Denmark Strait Overflow Water in a high-resolution numerical model hindcast simulation. *Journal of Geophysical Research: Oceans*, 122, 2830–2846. <https://doi.org/10.1002/2016JC012158>

Berglund, S., Döös, K., & Nylander, J. (2017). Lagrangian tracing of the water-mass transformations in the Atlantic Ocean. *Tellus, Series A: Dynamic meteorology and oceanography*, 69(1), 1–15. <https://doi.org/10.1080/16000870.2017.1306311>

Biastoch, A., Böning, C. W., Schwarzkopf, F. U., & Lutjeharms, J. R. E. (2009). Increase in Agulhas leakage due to poleward shift of Southern Hemisphere westerlies. *Nature*, 462, 495–498. <https://doi.org/10.1038/nature08519>

Biastoch, A., Durgadoo, J. V., Morrison, A. K., Van Sebille, E., Weijer, W., & Griffies, S. M. (2015). Atlantic multi-decadal oscillation covaries with Agulhas leakage. *Nature Communications*, 6(1), 10082. <https://doi.org/10.1038/ncomms10082>

Boebel, O., Davis, R. E., Ollitrault, M., Peterson, R. G., Richardson, P. L., Schmid, C., & Zenk, W. (1999). The intermediate depth circulation of the western South Atlantic. *Geophysical Research Letters*, 26(21), 3329–3332. <https://doi.org/10.1029/1999GL002355>

Boebel, O., Lutjeharms, J., Schmid, C., Zenk, W., Rossby, T., & Barron, C. (2003). The Cape Cauldron: a regime of turbulent inter-ocean exchange. *Deep Sea Research Part II: Topical Studies in Oceanography*, 50(1), 57–86. [https://doi.org/10.1016/S0967-0645\(02\)00379-X](https://doi.org/10.1016/S0967-0645(02)00379-X)

Bower, A., Furey, H., & Lozier, S. (2017). Overflow water pathways in the subpolar North Atlantic observed with deep floats. In EGU General Assembly Conference Abstracts (Vol. 19, p. 8103).

Bower, A., Lozier, S., & Gary, S. (2011). Export of Labrador Sea water from the subpolar North Atlantic: a Lagrangian perspective. *Deep Sea Research Part II: Topical Studies in Oceanography*, 58(17–18), 1798–1818. <https://doi.org/10.1016/j.dsr2.2010.10.060>

Bower, A. S. (1991). A Simple kinematic mechanism for mixing fluid parcels across a meandering jet. *Journal of Physical Oceanography*, 21(1), 173–180. [https://doi.org/10.1175/1520-0485\(1991\)021<0173:ASKMFM>2.0.CO;2](https://doi.org/10.1175/1520-0485(1991)021<0173:ASKMFM>2.0.CO;2)

Bower, A. S., Hendry, R. M., Amrhein, D. E., & Lilly, J. M. (2013). Direct observations of formation and propagation of subpolar eddies into the Subtropical North Atlantic. *Deep Sea Research Part II: Topical Studies in Oceanography*, 85, 15–41. <https://doi.org/10.1016/j.dsr2.2012.07.029>

Bower, A. S., & Hunt, H. D. (2000a). Lagrangian observations of the Deep Western Boundary Current in the North Atlantic Ocean. Part I: Large-scale pathways and spreading rates. *Journal of Physical Oceanography*, 30(5), 764–783. [https://doi.org/10.1175/1520-0485\(2000\)030<0764:LOOTDW>2.0.CO;2](https://doi.org/10.1175/1520-0485(2000)030<0764:LOOTDW>2.0.CO;2)

Bower, A. S., & Hunt, H. D. (2000b). Lagrangian observations of the Deep Western Boundary Current in the North Atlantic Ocean. Part II: The Gulf Stream-Deep Western Boundary Current crossover. *Journal of Physical Oceanography*, 30(5), 784–804. [https://doi.org/10.1175/1520-0485\(2000\)030<0784:LOOTDW>2.0.CO;2](https://doi.org/10.1175/1520-0485(2000)030<0784:LOOTDW>2.0.CO;2)

Bower, A. S., le Cann, B., Rossby, T., Zenk, W., Gould, J., Speer, K., et al. (2002). Directly measured mid-depth circulation in the north-eastern North Atlantic Ocean. *Nature*, 419(6907), 603–607. <https://doi.org/10.1038/nature01078>

Bower, A. S., & Lozier, M. S. (1994). A closer look at particle exchange in the Gulf Stream. *Journal of Physical Oceanography*, 24(6), 1399–1418. [https://doi.org/10.1175/1520-0485\(1994\)024<1399:ACLAPE>2.0.CO;2](https://doi.org/10.1175/1520-0485(1994)024<1399:ACLAPE>2.0.CO;2)

Bower, A. S., Lozier, M. S., Gary, S. F., & Böning, C. W. (2009). Interior pathways of the North Atlantic Meridional Overturning Circulation. *Nature*, 459(7244), 243–247. <https://doi.org/10.1038/nature07979>

Bower, A. S., & Rossby, H. T. (1989). Evidence of cross-frontal exchange processes in the Gulf Stream based on isopycnal RAFOS float data. *Journal of Physical Oceanography*, 19(9), 1177–1190. [https://doi.org/10.1175/1520-0485\(1989\)019<1177:EOCFEP>2.0.CO;2](https://doi.org/10.1175/1520-0485(1989)019<1177:EOCFEP>2.0.CO;2)

Brambilla, E., & Talley, L. D. (2006). Surface drifter exchange between the North Atlantic subtropical and subpolar gyres. *Journal of Geophysical Research*, 111, C07026. <https://doi.org/10.1029/2005JC003146>

Broecker, W. S. (1991). The Great Ocean Conveyor. *Oceanography*, 4(2), 79–89. <https://doi.org/10.5670/oceanog.1991.07>

Bryden, H. L., Longworth, H. R., & Cunningham, S. A. (2005). Slowing of the Atlantic Meridional Overturning Circulation at 25 N. *Nature*, 438(7068), 655–657. <https://doi.org/10.1038/nature04385>

Burkholder, K. C., & Lozier, M. S. (2011a). Mid-depth Lagrangian pathways in the North Atlantic and their impact on the salinity of the eastern subpolar gyre. *Deep-Sea Research I*, 58(12), 1196–1204. <https://doi.org/10.1016/j.dsr.2011.08.007>

Burkholder, K. C., & Lozier, M. S. (2011b). Subtropical to subpolar pathways in the North Atlantic: Deductions from Lagrangian trajectories. *Journal of Geophysical Research*, 116, C07017. <https://doi.org/10.1029/2010JC006697>

Burkholder, K. C., & Lozier, M. S. (2014). Tracing the pathways of the upper limb of the North Atlantic Meridional Overturning Circulation. *Geophysical Research Letters*, 41, 4254–4260. <https://doi.org/10.1002/2014GL060226>

Casal, T. G. D., Beal, L. M., & Lumpkin, R. (2006). A North Atlantic deep-water eddy in the Agulhas Current system. *Deep Sea Research I*, 53(10), 1718–1728. <https://doi.org/10.1016/j.dsr.2006.08.007>

Casanova-Masjoan, M., Pelegri, J. L., Sangrà, P., Martínez, A., Grisolía-Santos, D., Pérez-Hernández, M. D., & Hernández-Guerra, A. (2017). Characteristics and evolution of an Agulhas ring. *Journal of Geophysical Research: Oceans*, 122, 7049–7065. <https://doi.org/10.1002/2017JC012969>

Chenillat, F., Blanke, B., Grima, N., Franks, P. J. S., Capet, X., & Rivièvre, P. (2015). Quantifying tracer dynamics in moving fluids: A combined Eulerian-Lagrangian approach. *Frontiers in Environmental Science*, 3, 43. <https://doi.org/10.3389/fenvs.2015.00043>

Cunningham, S. A., Baringer, M. O., Johns, B., Toole, J., Østerhus, S., Fischer, J., et al. (2010). The present and future system for measuring the Atlantic Meridional Overturning Circulation and heat transport. In J. Hall, D. E. Harrison, & D. Stammer (Eds.), *Proceedings of OceanObs'09: Sustained Ocean Observations and Information for Society (Vol. 2)*, Venice, Italy, 21–25 September 2009, ESA Publication WPP-306 (pp. 229–244). Noordwijk, The Netherlands: European Space Agency. <https://doi.org/10.5270/OceanObs09.cwp.21>

Cunningham, S. A., Alderson, S. G., King, B. A., & Brandon, M. A. (2003). Transport and variability of the Antarctic Circumpolar Current in Drake Passage. *Journal of Geophysical Research*, 108(C5), 8084. <https://doi.org/10.1029/2001JC001147>

Cunningham, S. A., Kanzow, T., Rayner, D., Baringer, M. O., Johns, W. E., Marotzke, J., et al. (2007). Temporal variability of the Atlantic Meridional Overturning Circulation at 26.5 N. *Science*, 317(5840), 935–938. <https://doi.org/10.1126/science.1141304>

Cuny, J., Rhines, P. B., Niiler, P. P., & Bacon, S. (2002). Labrador Sea boundary currents and the fate of the Irminger Sea Water. *Journal of Physical Oceanography*, 32(2), 627–647. [https://doi.org/10.1175/1520-0485\(2002\)032<0627:LSBCAT>2.0.CO;2](https://doi.org/10.1175/1520-0485(2002)032<0627:LSBCAT>2.0.CO;2)

Daniault, N., Mercier, H., Lherminier, P., Sarafanov, A., Falina, A., Zunino, P., et al. (2016). The northern North Atlantic Ocean mean circulation in the early 21st century. *Progress in Oceanography*, 146, 142–158. <https://doi.org/10.1016/j.pocean.2016.06.007>

Davis, R. E., Regier, L. A., Dufour, J., & Webb, D. C. (1992). The autonomous Lagrangian circulation explorer (ALACE). *Journal of Atmospheric and Oceanic Technology*, 9(3), 264–285. [https://doi.org/10.1175/1520-0426\(1992\)009<0264:TALCE>2.0.CO;2](https://doi.org/10.1175/1520-0426(1992)009<0264:TALCE>2.0.CO;2)

de Jong, M. F., Soiland, H., Bower, A. S., & Furey, H. H. (2018). The subsurface circulation of the Iceland Sea observed with RAFOS floats. *Deep Sea Research Part I: Oceanographic Research Papers*, 141, 1–10. <https://doi.org/10.1016/j.dsr.2018.07.008>

Dengler, M., Schott, F. A., Eden, C., Brandt, P., Fischer, J., & Zantopp, R. J. (2004). Break-up of the Atlantic deep western boundary current into eddies at 8°S. *Nature*, 432(7020), 1018–1020. <https://doi.org/10.1038/nature03134>

Desbruyères, D., Mercier, H., & Thierry, V. (2015). On the mechanisms behind decadal heat content changes in the eastern subpolar gyre. *Progress in Oceanography*, 132, 262–272. <https://doi.org/10.1016/j.pocean.2014.02.005>

Desbruyères, D., Thierry, V., & Mercier, H. (2013). Simulated decadal variability of the meridional overturning circulation across the A25-Ovide section. *Journal of Geophysical Research: Oceans*, 118, 462–475. <https://doi.org/10.1029/2012JC008342>

Dickson, B., Dye, S., Jónsson, S., Köhl, A., Macrander, A., Marnela, M., et al. (2008). The overflow flux west of Iceland: Variability, origins and forcing. In *Arctic–Subarctic Ocean Fluxes* (pp. 443–474). Dordrecht: Springer.

Donners, J., & Drijfhout, S. S. (2004). The Lagrangian view of South Atlantic interocean exchange in a global ocean model compared with inverse model results. *Journal of Physical Oceanography*, 34(5), 1019–1035. [https://doi.org/10.1175/1520-0485\(2004\)034<1019:TLVOSA>2.0.CO;2](https://doi.org/10.1175/1520-0485(2004)034<1019:TLVOSA>2.0.CO;2)

Donohue, K. A., Tracey, K. L., Watts, D. R., Chidichimo, M. P., & Chereskin, T. K. (2016). Mean Antarctic Circumpolar Current transport measured in Drake Passage. *Geophysical Research Letters*, 43, 11,760–11,767. <https://doi.org/10.1002/2016GL070319>

Durgadoo, J. V., Loveday, B. R., Reason, C. J. C., Penven, P., & Biastoch, A. (2013). Agulhas leakage predominantly responds to the Southern Hemisphere westerlies. *Journal of Physical Oceanography*, 43(10), 2113–2131. <https://doi.org/10.1175/JPO-D-13-047.1>

Durgadoo, J. V., Rühs, S., Biastoch, A., & Böning, C. W. B. (2017). Indian Ocean sources of Agulhas leakage. *Journal of Geophysical Research: Oceans*, 122, 3481–3499. <https://doi.org/10.1002/2016JC012676>

Fischer, J., & Schott, F. A. (2002). Labrador Sea Water tracked by profiling floats—From the boundary current into the open North Atlantic. *Journal of Physical Oceanography*, 32(2), 573–584. [https://doi.org/10.1175/1520-0485\(2002\)032<0573:LSWTBP>2.0.CO;2](https://doi.org/10.1175/1520-0485(2002)032<0573:LSWTBP>2.0.CO;2)

Flatau, M. K., Talley, L., & Niiler, P. P. (2003). The North Atlantic Oscillation, surface current velocities, and SST changes in the subpolar North Atlantic. *Journal of Climate*, 16(14), 2355–2369. <https://doi.org/10.1175/2787.1>

Foukal, N. P., & Lozier, M. S. (2016). No inter-gyre pathway for sea-surface temperature anomalies in the North Atlantic. *Nature Communications*, 7(1). <https://doi.org/10.1038/ncomms1133>

Foukal, N. P., & Lozier, M. S. (2018). Examining the origins of ocean heat content variability in the eastern North Atlantic Subpolar Gyre. *Geophysical Research Letters*, 45, 11,275–11,283. <https://doi.org/10.1029/2018GL079122>

Fratantoni, D. M. (2001). North Atlantic surface circulation during the 1990s observed with satellite-tracked drifters. *Journal of Geophysical Research*, 106(C10), 22,067–22,093. <https://doi.org/10.1029/2000JC000730>

Fratantoni, D. M., Johns, W. E., Townsend, T. L., & Hurlburt, H. E. (2000). Low-latitude circulation and mass transport pathways in a model of the tropical Atlantic Ocean. *Journal of Physical Oceanography*, 30(8), 1944–1966. [https://doi.org/10.1175/1520-0485\(2000\)030<1944:LLCAMT>2.0.CO;2](https://doi.org/10.1175/1520-0485(2000)030<1944:LLCAMT>2.0.CO;2)

Fratantoni, D. M., Kwon, Y.-O., & Hodges, B. A. (2013). Direct observation of subtropical mode water circulation in the western North Atlantic Ocean. *Deep Sea Research Part II: Topical Studies in Oceanography*, 91, 35–56. <https://doi.org/10.1016/j.dsrr.2013.02.027>

Fratantoni, D. M., & Richardson, P. L. (2006). The evolution and demise of North Brazil Current rings. *Journal of Physical Oceanography*, 36(7), 1241–1264. <https://doi.org/10.1175/JPO2907.1>

Friocourt, Y., Drijfhout, S., Blanke, B., & Speich, S. (2005). Water mass export from Drake Passage to the Atlantic, Indian, and Pacific Oceans: A Lagrangian model analysis. *Journal of Physical Oceanography*, 35(7), 1206–1222. <https://doi.org/10.1175/JPO2748.1>

Funk, A., Brandt, P., & Fischer, T. (2009). Eddy diffusivities estimated from observations in the Labrador Sea. *Journal of Geophysical Research*, 114, C04001. <https://doi.org/10.1029/2008JC005098>

Gary, S. F., Lozier, M. S., Biastoch, A., Böning, C. W. (2012). Reconciling tracer and float observations of the export pathways of Labrador Sea Water. *Geophysical Research Letters*, 39, L24606. <https://doi.org/10.1029/2012GL053978>

Gary, S. F., Lozier, M. S., Böning, C. W., & Biastoch, A. (2011). Deciphering the pathways for the deep limb of the Meridional Overturning Circulation. *Deep Sea Research Part II: Topical Studies in Oceanography*, 58(17–18), 1781–1797. <https://doi.org/10.1016/j.dsrr.2010.10.059>

Gary, S. F., Lozier, M. S., Kwon, Y.-O., & Park, J. J. (2014). The fate of North Atlantic subtropical mode water in the FLAME model. *Journal of Physical Oceanography*, 44(5), 1354–1371. <https://doi.org/10.1175/JPO-D-13-0202.1>

Garzoli, S. L., Dong, S., Fine, R., Meinen, C. S., Perez, R. C., Schmid, C., et al. (2015). The fate of the Deep Western Boundary Current in the South Atlantic. *Deep Sea Research Part I: Oceanographic Research Papers*, 103, 125–136. <https://doi.org/10.1016/j.dsri.2015.05.008>

Garzoli, S. L., & Matano, R. (2011). The South Atlantic and the Atlantic Meridional Overturning Circulation. *Deep Sea Research Part II: Topical Studies in Oceanography*, 58, 1837–1847. <https://doi.org/10.1016/j.dsrr.2010.10.063>

Getzlaff, K., Böning, C. W., & Dengg, J. (2006). Lagrangian perspectives of deep water export from the subpolar North Atlantic. *Geophysical Research Letters*, 33, L21S08. <https://doi.org/10.1029/2006GL026470>

Gordon, A. L. (1989). Brazil–Malvinas Confluence–1984. *Deep Sea Research Part A: Oceanographic Research Papers*, 36(3), 359–384. [https://doi.org/10.1016/0198-0149\(89\)90042-3](https://doi.org/10.1016/0198-0149(89)90042-3)

Gould, W. J. (2005). From swallow floats to Argo—The development of neutrally buoyant floats. *Deep Sea Research Part II: Topical Studies in Oceanography*, 52(3–4), 529–543. <https://doi.org/10.1016/j.dsrr.2004.12.005>

Häkkinen, S., & Rhines, P. B. (2009). Shifting surface currents in the northern North Atlantic Ocean. *Journal of Geophysical Research*, 114, C04005. <https://doi.org/10.1029/2008JC004883>

Häkkinen, S., Rhines, P. B., & Worthen, D. L. (2011). Warm and saline events embedded in the meridional circulation of the northern North Atlantic. *Journal of Geophysical Research*, 116, C03006. <https://doi.org/10.1029/2010JC006275>

Halliwell, G. R. Jr., Weisberg, R. H., & Mayer, D. A. (2003). A synthetic float analysis of upper-limb meridional overturning circulation interior. *Interhemispheric Water Exchange in the Atlantic Ocean*, 68, 93. [https://doi.org/10.1016/S0422-9894\(03\)80144-7](https://doi.org/10.1016/S0422-9894(03)80144-7)

Hogg, N. G., & Owens, W. B. (1999). Direct measurement of the deep circulation within the Brazil Basin. *Deep Sea Research Part II: Topical Studies in Oceanography*, 46(1–2), 335–353. <https://doi.org/10.1029/2004JC002311>

Howe, B., J. Miksis-Olds, E. Rehm, H. Sagen, P. Worcester, & G. Haralabus (2019). Observing the Oceans Acoustically. *Frontiers in Marine Science*, manuscript in review.

Intergovernmental Panel on Climate Change Fifth Assessment Report (2014). In Core Writing Team, R. K. Pachauri, & L. A. Meyer (Eds.), *Climate change 2014: Synthesis report. Contribution of Working Groups I, II and III to the Fifth Assessment Report of the Intergovernmental Panel on Climate Change*, (p. 151). Geneva, Switzerland: IPCC.

Jakobsen, P. K., Røberggaard, M. H., Quadfasel, D., Schmitt, T., & Hughes, C. W. (2003). Near-surface circulation in the northern North Atlantic as inferred from Lagrangian drifters: Variability from the mesoscale to interannual. *Journal of Geophysical Research*, 108(C8), 3251. <https://doi.org/10.1029/2002JC001554>

Jonsson, S., & Valdimarsson, H. (2004). A new path for the Denmark Strait overflow water from the Iceland Sea to Denmark Strait. *Geophysical Research Letters*, 31, L03305. <https://doi.org/10.1029/2003GL019214>

Kanzow, T., & Zenk, W. (2014). Structure and transport of the Iceland Scotland Overflow plume along the Reykjanes Ridge in the Iceland Basin. *Deep Sea Research Part I: Oceanographic Research Papers*, 86, 82–93. <https://doi.org/10.1016/j.dsr.2013.11.003>

Köhle, A. (2010). Variable source regions of Denmark Strait and Faroe Bank Channel overflow waters. *Tellus A: Dynamic Meteorology and Oceanography*, 62(4), 551–568. <https://doi.org/10.1111/j.1600-0870.2010.00454.x>

Koszalka, I., LaCasce, J. H., Andersson, M., Orvik, K. A., & Mauritzen, C. (2011). Surface circulation in the Nordic Seas from clustered drifters. *Deep Sea Research Part I: Oceanographic Research Papers*, 58(4), 468–485. <https://doi.org/10.1016/j.dsr.2011.01.007>

Koszalka, I. M., Haine, T. W., & Magaldi, M. G. (2013). Fates and travel times of Denmark Strait overflow water in the Irminger Basin. *Journal of Physical Oceanography*, 43(12), 2611–2628. <https://doi.org/10.1175/JPO-D-13-023.1>

Kwon, Y., Park, J., Gary, S. F., & Lozier, M. S. (2015). Year-to-year reoutcropping of eighteen degree water in an eddy-resolving oceans simulation. *Journal of Physical Oceanography*, 45(4), 1189–1204. <https://doi.org/10.1175/JPO-D-14-0122.1>

Kwon, Y.-O., & Riser, S. C. (2005). General circulation of the western subtropical North Atlantic observed using profiling floats. *Journal of Geophysical Research*, 110, C10012. <https://doi.org/10.1029/2005JC002909>

Lankhorst, M., Fratantoni, D., Ollitrault, M., Richardson, P., Send, U., & Zenk, W. (2009). The mid-depth circulation of the northwestern tropical Atlantic observed by floats. *Deep Sea Research Part I: Oceanographic Research Papers*, 56(10), 1615–1632. <https://doi.org/10.1016/j.dsr.2009.06.002>

Lankhorst, M., & Zenk, W. (2006). Lagrangian observations of the middepth and deep velocity fields of the northeastern Atlantic Ocean. *Journal of Physical Oceanography*, 36(1), 43–63. <https://doi.org/10.1175/JPO2869.1>

Lavender, K. L., Davis, R. E., & Owens, W. B. (2000). Mid-depth recirculation observed in the interior Labrador and Irminger seas by direct velocity measurements. *Nature*, 407(6800), 66–69. <https://doi.org/10.1038/35024048>

Leaman, K. D., & Vertes, P. S. (1996). Topographic influences on recirculation in the deep western boundary current: results from RAFOS float trajectories between the Blake–Bahama Outer Ridge and the San Salvador “Gate”. *Journal of Physical Oceanography*, 26(6), 941–961. [https://doi.org/10.1175/1520-0485\(1996\)026<941:TIORIT>2.0.CO;2](https://doi.org/10.1175/1520-0485(1996)026<941:TIORIT>2.0.CO;2)

Lique, C., Treguier, A. M., Blanke, B., & Grima, N. (2010). On the origins of water masses exported along both sides of Greenland: A Lagrangian model analysis. *Journal of Geophysical Research*, 115, C05019. <https://doi.org/10.1029/2009JC005316>

Lozier, M. S. (1997). Evidence for large-scale eddy-driven gyres in the North Atlantic. *Science*, 277(5324), 361–364. <https://doi.org/10.1126/science.277.5324.361>

Lozier, M. S. (1999). The impact of middepth recirculations on the distribution of tracers in the North Atlantic. *Geophysical Research Letters*, 26(2), 219–222. <https://doi.org/10.1029/1998GL900264>

Lozier, M. S., Bacon, S., Bower, A. S., Cunningham, S. A., Femke de Jong, M., de Steur, L., et al. (2017). Overturning in the Subpolar North Atlantic Program: a new international ocean observing system. *Bulletin of the American Meteorological Society*, 98(4), 737–752. <https://doi.org/10.1175/BAMS-D-16-0057.1>

Lozier, M. S., & Bercovici, D. (1992). Particle exchange in an unstable jet. *Journal of Physical Oceanography*, 22(12), 1506–1516. [https://doi.org/10.1175/1520-0485\(1992\)022<1506:PEIAUJ>2.0.CO;2](https://doi.org/10.1175/1520-0485(1992)022<1506:PEIAUJ>2.0.CO;2)

Lozier, M. S., Gary, S. F., & Bower, A. S. (2013). Simulated pathways of the overflow waters in the North Atlantic: Subpolar to subtropical export. *Deep Sea Research Part II: Topical Studies in Oceanography*, 85, 147–153. <https://doi.org/10.1016/j.dsr2.2012.07.037>

Lozier, M. S., Li, F., Bacon, S., Bahr, F., Bower, A. S., Cunningham, S. A., et al. (2019). A seachange in our view of overturning in the subpolar North Atlantic. *Science*, 363(6426), 516–521.

Lozier, M. S., & Riser, S. C. (1989). Potential vorticity dynamics of boundary currents in a quasigeostrophic ocean. *Journal of Physical Oceanography*, 19(9), 1373–1396. [https://doi.org/10.1175/1520-0485\(1989\)019<1373:PVDOBC>2.0.CO;2](https://doi.org/10.1175/1520-0485(1989)019<1373:PVDOBC>2.0.CO;2)

Lozier, M. S., & Stewart, N. M. (2008). On the temporally varying northward penetration of Mediterranean Overflow Water and eastward penetration of Labrador Sea Water. *Journal of Physical Oceanography*, 38(9), 2097–2103. <https://doi.org/10.1175/2008JPO3908.1>

Lumpkin, R., & Garzoli, S. L. (2005). Near-surface circulation in the tropical Atlantic Ocean. *Deep Sea Research Part I: Oceanographic Research Papers*, 52(3), 495–518. <https://doi.org/10.1016/j.dsr.2004.09.001>

Lumpkin, R., & Johnson, G. C. (2013). Global ocean surface velocities from drifters: Mean, variance, El Niño–Southern Oscillation response, and seasonal cycle. *Journal of Geophysical Research: Oceans*, 118, 2992–3006. <https://doi.org/10.1002/jgrc.20210>

Marsh, R., Haigh, I. D., Cunningham, A. A., Inall, M. E., Porter, M., & Moat, B. I. (2017). Large-scale forcing of the European Slope Current and associated inflows to the North Sea. *Ocean Science*, 13(2), 315–335. <https://doi.org/10.5194/os-13-315-2017>

Maximenko, N., Niiler, P., Centurioni, L., Rio, M. H., Melnichenko, O., Chambers, D., et al. (2009). Mean dynamic topography of the ocean derived from satellite and drifting buoy data using three different techniques. *Journal of Atmospheric and Oceanic Technology*, 26(9), 1910–1919. <https://doi.org/10.1175/2009JTECHO672.1>

McCarthy, G. D., Smeed, D. A., Johns, W. E., Frajka-Williams, E., Moat, B. I., Rayner, D., et al. (2015). Measuring the Atlantic Meridional Overturning Circulation at 26 N. *Progress in Oceanography*, 130, 91–111. <https://doi.org/10.1016/j.pocean.2014.10.006>

McClean, J. L., Poulain, P. M., Pelton, J. W., & Maitrud, M. E. (2002). Eulerian and Lagrangian statistics from surface drifters and a high-resolution POP simulation in the North Atlantic. *Journal of Physical Oceanography*, 32(9), 2472–2491. <https://doi.org/10.1175/1520-0485-32.9.2472>

Meinen, C. S., Speich, S., Piola, A. R., Ansorge, I., Campos, E., Kersalé, M., et al. (2018). Meridional Overturning Circulation transport variability at 34.5° S during 2009–2017: Baroclinic and barotropic flows and the dueling influence of the boundaries. *Geophysical Research Letters*, 45, 4180–4188. <https://doi.org/10.1029/2018GL077408>

Mercier, H., Lherminier, P., Sarafanov, A., Gaillard, F., Daniault, N., Desbruyères, D., et al. (2015). Variability of the meridional overturning circulation at the Greenland–Portugal OVIDE section from 1993 to 2010. *Progress in Oceanography*, 132, 250–261. <https://doi.org/10.1016/j.pocean.2013.11.001>

Ollitrault, M., Lankhorst, M., Fratantoni, D., Richardson, P., & Zenk, W. (2006). Zonal intermediate currents in the equatorial Atlantic Ocean. *Geophysical Research Letters*, 33, L05605. <https://doi.org/10.1029/2005GL025368>

Orvik, K. A., & Niiler, P. (2002). Major pathways of Atlantic water in the northern North Atlantic and Nordic Seas toward Arctic. *Geophysical Research Letters*, 29(19), 1896. <https://doi.org/10.1029/2002GL015002>

Owens, W. B. (1991). A statistical description of the mean circulation and eddy variability in the northwestern Atlantic using SOFAR floats. *Progress in Oceanography*, 28(3), 257–303. [https://doi.org/10.1016/0079-6611\(91\)90010-J](https://doi.org/10.1016/0079-6611(91)90010-J)

Palter, J. B., & Lozier, M. S. (2008). On the source of Gulf Stream nutrients. *Journal of Geophysical Research*, 113, C06018. <https://doi.org/10.1029/2007JC004611>

Pickart, R. S., Torres, D. J., & Fratantoni, P. S. (2005). The east Greenland spill jet. *Journal of Physical Oceanography*, 35(6), 1037–1053. <https://doi.org/10.1175/JPO2734.1>

Poulain, P. M., Warn-Varnas, A., & Niiler, P. P. (1996). Near-surface circulation of the Nordic seas as measured by Lagrangian drifters. *Journal of Geophysical Research*, 101(C8), 18,237–18,258. <https://doi.org/10.1029/96JC00506>

Prater, M. D. (2002). Eddies in the Labrador Sea as observed by profiling RAFOS floats and remote sensing. *Journal of Physical Oceanography*, 32(2), 411–427. [https://doi.org/10.1175/1520-0485\(2002\)032<0411:EITLSA>2.0.CO;2](https://doi.org/10.1175/1520-0485(2002)032<0411:EITLSA>2.0.CO;2)

Prater, M. D., & Rossby, T. (2005). Observations of the Faroe Bank Channel overflow using bottom-following RAFOS floats. *Deep Sea Research Part II: Topical Studies in Oceanography*, 52(3-4), 481–494. <https://doi.org/10.1016/j.dsrt.2004.12.009>

Ramsey, A., Furey, H., & Bower, A. (2018). Deep floats reveal complex ocean circulation patterns. *Eos*, 99. <https://doi.org/10.1029/2018EO105549>

Rhein, M., Fischer, J., Smethie, W. M., Smythe-Wright, D., Weiss, R. F., Mertens, C., et al. (2002). Labrador Sea Water: Pathways, CFC inventory, and formation rates. *Journal of Physical Oceanography*, 32(2), 648–665. [https://doi.org/10.1175/1520-0485\(2002\)032<0648:LSWPCI>2.0.CO;2](https://doi.org/10.1175/1520-0485(2002)032<0648:LSWPCI>2.0.CO;2)

Ribergaard, M.H. (2004). On the coupling between hydrography and larval transport in the Southwest Greenland waters. Ph.D. thesis. University of Copenhagen. Re-issued as DMI scientific report, 05-05.

Richardson, P. L. (1992). Velocity and eddy kinetic energy of the Gulf Stream system from 700-m SOFAR floats subsampled to simulate pop-up floats. *Journal of Atmospheric and Oceanic Technology*, 9(4), 495–503. [https://doi.org/10.1175/1520-0426\(1992\)009<0495:VAEKEO>2.0.CO;2](https://doi.org/10.1175/1520-0426(1992)009<0495:VAEKEO>2.0.CO;2)

Richardson, P. L. (2007). Agulhas leakage into the Atlantic estimated with subsurface floats and surface drifters. *Deep Sea Research Part I: Oceanographic Research Papers*, 54(8), 1361–1389. <https://doi.org/10.1016/j.dsri.2007.04.010>

Richardson, P. L. (2019). Drifters and floats. In J. K. Cochran, H. J. Bokuniewicz, & P. L. Yager (Eds.), *Encyclopedia of Ocean Sciences* (3rd ed., pp. 63–70). New York: Elsevier.

Richardson, P. L., & Fratantoni, D. M. (1999). Float trajectories in the deep western boundary current and deep equatorial jets of the tropical Atlantic. *Deep Sea Research Part II: Topical Studies in Oceanography*, 46(1-2), 305–333. [https://doi.org/10.1016/S0967-0645\(98\)00100-3](https://doi.org/10.1016/S0967-0645(98)00100-3)

Richardson, P. L., & Schmitz, W. J. Jr. (1993). Deep cross-equatorial flow in the Atlantic measured with SOFAR floats. *Journal of Geophysical Research*, 98(C5), 8371–8387. <https://doi.org/10.1029/93JC00051>

Rimaud, J., Speich, S., Blanke, B., & Grima, N. (2012). The exchange of Intermediate Water in the southeast Atlantic: Water mass transformations diagnosed from the Lagrangian analysis of a regional ocean model. *Journal of Geophysical Research*, 117, C08034. <https://doi.org/10.1029/2012JC008059>

Rintoul, S. R. (1991). South Atlantic interbasin exchange. *Journal of Geophysical Research*, 96(C2), 2675–2692. <https://doi.org/10.1029/90JC02422>

Rodrigues, R. R., Wimbush, M., Watts, D. R., Rothstein, L. M., & Ollitrault, M. (2010). South Atlantic mass transports obtained from subsurface float and hydrographic data. *Journal of Marine Research*, 68, 819–850. <https://doi.org/10.1357/002224010796673858>

Rossby, T. (2016). Visualizing and quantifying oceanic motion. *Annual review of Marine Science*, 8(1), 35–57. <https://doi.org/10.1146/annurev-marine-122414-033849>

Rossby, T., Dorson, D., & Fontaine, J. (1986). The RAFOS system. *Journal of Oceanic and Atmospheric Technology*, 3(4), 672–679. [https://doi.org/10.1175/1520-0426\(1986\)003<0672:TRS>2.0.CO;2](https://doi.org/10.1175/1520-0426(1986)003<0672:TRS>2.0.CO;2)

Rossby, T., Flagg, C., Chafik, L., Harden, B., & Søiland, H. (2018). A direct estimate of volume, heat, and freshwater exchange across the Greenland-Iceland-Faroe-Scotland Ridge. *Journal of Geophysical Research: Oceans*, 123, 7139–7153. <https://doi.org/10.1029/2018JC014250>

Rossby, T., Prater, M. D., & Søiland, H. (2009). Pathways of inflow and dispersion of warm waters in the Nordic seas. *Journal of Geophysical Research*, 114, C04011. <https://doi.org/10.1029/2008JC005073>

Rossby, T., & Webb, D. (1970). Observing abyssal motions by tracking Swallow floats in the SOFAR channel. In *Deep Sea Research and Oceanographic Abstracts* (Vol. 17, No. 2, pp. 359–365). New York: Elsevier.

Rühs, S., Durgadoo, J. V., Behrens, E., & Biastoch, A. (2013). Advective timescales and pathways of Agulhas leakage. *Geophysical Research Letters*, 40, 3997–4000. <https://doi.org/10.1002/grl.50782>

Rühs, S., Schwarzkopf, F. U., Speich, S., & Biastoch, A. (2019). Cold vs. warm water route – sources for the upper limb of the Atlantic Meridional Overturning Circulation revisited in a high-resolution ocean model. *Ocean Science*, 15(3), 489–512. <https://doi.org/10.5194/os-15-489-2019>

Rusciano, E., Speich, S., & Ollitrault, M. (2012). Intercean exchanges and the spreading of Antarctic Intermediate Water south of Africa. *Journal of Geophysical Research*, 117, C10010. <https://doi.org/10.1029/2012JC008266>

Sarafanov, A., Falina, A., Mercier, H., Sokov, A., Lherminier, P., Gourcuff, C., et al. (2012). Mean full-depth summer circulation and transports at the northern periphery of the Atlantic Ocean in the 2000s. *Journal of Geophysical Research*, 117, C01014. <https://doi.org/10.1029/2011JC007572>

Schmitz, W. J., Luyten, J. R., & Schmitt, R. W. (1993). On the Florida Current T/S envelope. *Bulletin of Marine Science*, 53, 1048–1065.

Schmitz, W. J., & McCartney, M. S. (1993). On the North Atlantic circulation. *Reviews of Geophysics*, 31, 29–49. <https://doi.org/10.1029/92RG02583>

Schott, F. A., Fischer, J., Dengler, M., & Zantopp, R. (2006). Variability of the deep western boundary current east of the Grand Banks. *Geophysical Research Letters*, 33, L21S07. <https://doi.org/10.1029/2006GL026563>

Schott, F. A., Zantopp, R., Stramma, L., Dengler, M., Fischer, J., & Wibaux, M. (2004). Circulation and deep-water export at the western exit of the subpolar North Atlantic. *Journal of Physical Oceanography*, 34(4), 817–843. [https://doi.org/10.1175/1520-0485\(2004\)034<0817:CADEAT>2.0.CO;2](https://doi.org/10.1175/1520-0485(2004)034<0817:CADEAT>2.0.CO;2)

Send, U., Lankhorst, M., & Kanzow, T. (2011). Observation of decadal change in the Atlantic Meridional Overturning Circulation using 10 years of continuous transport data. *Geophysical Research Letters*, 38, L24606. <https://doi.org/10.1029/2011GL049801>

Sévellec, F., Colin de Verdiere, A., & Ollitrault, M. (2017). Evolution of intermediate water masses based on Argo float displacements. *Journal of Physical Oceanography*, 47(7), 1569–1586. <https://doi.org/10.1175/JPO-D-16-0182.1>

Shoosmith, D. R., Richardson, P. L., Bower, A. S., & Rossby, H. T. (2005). Discrete eddies in the northern North Atlantic as observed by looping RAFOS floats. *Deep Sea Research Part II: Topical Studies in Oceanography*, 52(3-4), 627–650. <https://doi.org/10.1016/j.dsrt.2004.12.011>

Smethie, W., Fine, R., Putzka, A., & Jones, E. (2000). Tracing the flow of North Atlantic Deep Water using chlorofluorocarbons. *Journal of Geophysical Research*, 105(C6), 14,297–14,323. <https://doi.org/10.1029/1999JC900274>

Søiland, H., Prater, M. D., & Rossby, T. (2008). Rigid topographic control of currents in the Nordic Seas. *Geophysical Research Letters*, 35, L18607. <https://doi.org/10.1029/2008GL034846>

Song, T., Rossby, T., & Carter, E. (1995). Lagrangian studies of fluid exchange between the Gulf Stream and surrounding waters. *Journal of Physical Oceanography*, 25(1), 46–63. [https://doi.org/10.1175/1520-0485\(1995\)025<0046:LSOFEB>2.0.CO;2](https://doi.org/10.1175/1520-0485(1995)025<0046:LSOFEB>2.0.CO;2)

Souza, J., de Boyer Montégut, C., Cabanes, C., & Klein, P. (2011). Estimation of the Agulhas ring impacts on meridional heat fluxes and transport using ARGO floats and satellite data. *Geophysical Research Letters*, 38, L21602. <https://doi.org/10.1029/2011GL049359>

Speich, S., Blanke, B., & Cai, W. (2007). Atlantic Meridional Overturning Circulation and the Southern Hemisphere supergyre. *Geophysical Research Letters*, 34, L23614. <https://doi.org/10.1029/2007GL031583>

Speich, S., Blanke, B., & Madec, G. (2001). Warm and cold water routes of an OGCM thermohaline conveyor belt. *Geophysical Research Letters*, 28(2), 311–314. <https://doi.org/10.1029/2000GL011748>

Srokosz, M. A., & Bryden, H. L. (2015). Observing the Atlantic Meridional Overturning Circulation yields a decade of inevitable surprises. *Science*, 348(6241), 1255575. <https://doi.org/10.1126/science.1255575>

Stommel, H. (1955). Direct measurements of sub-surface currents. *Deep Sea Research*, 2(4), 284–285. [https://doi.org/10.1016/0146-6313\(55\)90006-X](https://doi.org/10.1016/0146-6313(55)90006-X)

Stommel, H. (1957). A survey of ocean current theory. *Deep Sea Research*, 4, 149–184. [https://doi.org/10.1016/0146-6313\(56\)90048-X](https://doi.org/10.1016/0146-6313(56)90048-X)

Stommel, H., & Arons, A. B. (1960a). On the abyssal circulation of the world ocean part I: stationary planetary flow patterns on a sphere. *Deep-Sea Research*, 6, 140–154.

Stommel, H., & Arons, A. B. (1960b). On the abyssal circulation of the world ocean part II: an idealized model of the circulation pattern and amplitude in the oceanic basins. *Deep-Sea Research*, 6, 217–233.

Stommel, H. M. (1958). *The Gulf Stream: a physical and dynamical description*. Berkeley: University of California Press.

Swallow, J. C., & Worthington, L. V. (1957). Measurements of deep currents in the western North Atlantic. *Nature*, 179(4571), 1183–1184. <https://doi.org/10.1038/1791183b0>

Swallow, J. C., & Worthington, L. V. (1961). An observation of a deep countercurrent in the western North Atlantic. *Deep Sea Research*, 8(1), 1–IN3. [https://doi.org/10.1016/0146-6313\(61\)90011-9](https://doi.org/10.1016/0146-6313(61)90011-9)

Talley, L., & McCartney, M. (1982). Distribution and circulation of Labrador Sea water. *Journal of Physical Oceanography*, 12(11), 1189–1205. [https://doi.org/10.1175/1520-0485\(1982\)012<1189:DACOLS>2.0.CO;2](https://doi.org/10.1175/1520-0485(1982)012<1189:DACOLS>2.0.CO;2)

The CLIMODE Group (2009). The CLIMODE field campaign: Observing the cycle of convection and restratification over the Gulf Stream. *Bulletin of the American Meteorological Society*, 90(9), 1337–1350. <https://doi.org/10.1175/2009BAMS2706.1>

Toole, J., Andres, M., Le Bras, I., Joyce, T. M., & McCartney, M. S. (2017). Moored observations of the Deep Western Boundary Current in the NW Atlantic: 2004–2014. *Journal of Geophysical Research: Oceans*, 122, 7488–7505. <https://doi.org/10.1002/2017JC012984>

Trenberth, K. E., & Caron, J. M. (2001). Estimates of meridional atmosphere and ocean heat transports. *Journal of Climate*, 14(16), 3433–3443. [https://doi.org/10.1175/1520-0442\(2001\)014<3433:EOMAAO>2.0.CO;2](https://doi.org/10.1175/1520-0442(2001)014<3433:EOMAAO>2.0.CO;2)

Trenberth, K. E., & Fasullo, J. T. (2017). Atlantic meridional heat transports computed from balancing Earth's energy locally. *Geophysical Research Letters*, 44, 1919–1927. <https://doi.org/10.1002/2016GL072475>

Väge, K., Pickart, R. S., Spall, M. A., Valdimarsson, H., Jónsson, S., Torres, D. J., et al. (2011). Significant role of the North Icelandic Jet in the formation of Denmark Strait overflow water. *Nature Geoscience*, 4(10), 723–727. <https://doi.org/10.1038/ngeo1234>

Van Aken, H. M. (2000). The hydrography of the mid-latitude northeast Atlantic Ocean: I: The deep water masses. *Deep Sea Research Part I: Oceanographic Research Papers*, 47(5), 757–788.

van Aken, H. M., van Veldhoven, A. K., Veth, C., de Ruijter, W. P. M., van Leeuwen, P. J., Drijfhout, S. S., et al. (2003). Observations of a young Agulhas ring, Astrid, during MARE in March 2000. *Deep Sea Research Part II: Topical Studies in Oceanography*, 50(1), 167–195. [https://doi.org/10.1016/S0967-0645\(02\)00383-1](https://doi.org/10.1016/S0967-0645(02)00383-1)

van Sebille, E., Griffies, S. M., Abernathey, R., Adams, T. P., Berloff, P., Biastoch, A., et al. (2017). Lagrangian ocean analysis: fundamentals and practices. *Ocean Modelling*, 121, 49–75.

van Sebille, E., Johns, W. E., & Beal, L. M. (2012). Does the vorticity flux from Agulhas rings control the zonal pathway of NADW across the South Atlantic. *Journal of Geophysical Research*, 117, C05037. <https://doi.org/10.1029/2011JC007684>

Voet, G., Quadfasel, D., Mørk, K. A., & Søiland, H. (2010). The mid-depth circulation of the Nordic Seas derived from profiling float observations. *Tellus A: Dynamic Meteorology and Oceanography*, 62(4), 516–529. <https://doi.org/10.1111/j.1600-0870.2010.00444.x>

von Appen, W. J., Koszalka, I. M., Pickart, R. S., Haine, T. W. N., Mastropole, D., Magaldi, M. G., et al. (2014). The East Greenland Spill Jet as an important component of the Atlantic Meridional Overturning Circulation. *Deep Sea Research Part I: Oceanographic Research Papers*, 92, 75–84. <https://doi.org/10.1016/j.dsr.2014.06.002>

Weijer, W., De Ruijter, W. P., Sterl, A., & Drijfhout, S. S. (2002). Response of the Atlantic overturning circulation to South Atlantic sources of buoyancy. *Global and Planetary Change*, 34(3–4), 293–311.

Willis, J. (2010). Can in situ floats and satellite altimeters detect long-term changes in Atlantic Ocean overturning? *Geophysical Research Letters*, 37, L06602. <https://doi.org/10.1029/2010GL042372>

Worthington, L. (1958). The 188C water in the Sargasso Sea. *Deep Sea Research*, 5, 297–305. [https://doi.org/10.1016/0146-6313\(58\)90026-1](https://doi.org/10.1016/0146-6313(58)90026-1)

Xu, X., Schmitz, W. J., Hurlburt, H. E., & Hogan, P. J. (2012). Mean Atlantic Meridional Overturning Circulation across 26.5° N from eddy-resolving simulations compared to observations. *Journal of Geophysical Research*, 117, C03042. <https://doi.org/10.1029/2011JC007586>

Zantopp, R., Fischer, J., Visbeck, M., & Karstensen, J. (2017). From interannual to decadal: 17 years of boundary current transports at the exit of the Labrador Sea. *Journal of Geophysical Research: Oceans*, 122, 1724–1748. <https://doi.org/10.1002/2016JC012271>

Zhao, J., & Johns, W. (2014). Wind-forced interannual variability of the Atlantic Meridional Overturning Circulation at 26.5° N. *Journal of Geophysical Research: Oceans*, 119, 2403–2419. <https://doi.org/10.1002/2013JC009407>

Zou, S., & Lozier, M. S. (2016). Breaking the linkage between Labrador Sea Water production and its advective export to the subtropical gyre. *Journal of Physical Oceanography*, 46(7), 2169–2182. <https://doi.org/10.1175/JPO-D-15-0210.1>

Zou, S., Lozier, S., Zenk, W., Bower, A., & Johns, W. (2017). Observed and modeled pathways of the Iceland Scotland Overflow Water in the eastern North Atlantic. *Progress in Oceanography*, 159, 211–222. <https://doi.org/10.1016/j.pocean.2017.10.003>